Analysis of neutrino interactions for the search of supernova signals

Andrey Sheshukov

DLNP JINR

April 27, 2023

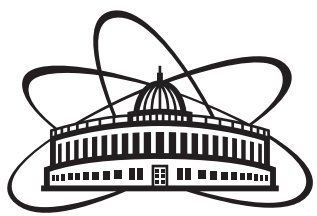

Outline

Stellar evolution phases

The stellar evolution is governed by hydrostatic burning of nuclear elements. Fuel element produces heavier elements in the stellar core. When the fuel in the central region is depleted, the burning stops, and the core contracts.

Stage	Time scale	Fuel	Product	T (10^9 K)	ρ (g/cm^3)
Hydrogen	11 My	H	He	0.035	5.8
Helium	2 My	He	C,O	0.018	1390
Carbon	2000 y	C	Ne,Mg	0.81	2.8×10^5
Neon	0.7 y	Ne	O,Mg	1.6	1.2×10^7
Oxygen	2.6 y	O,Mg	Si,S,Ar,Ca	1.9	8.8×10^6
Silicon	18 d	Si,S,Ar,Ca	Fe,Ni,Cr,Ti,...	3.3	4.8×10^7

Table: Stellar evolution phases for a 15 $M_\odot$ star from Woosley and H.-T. Janka 2005

Pre-supernova neutrino emission

Starting from the carbon core burning phase the energy loss by neutrino emission mostly via electron-positron pair annihilation and plasmon decay processes:

$$\begin{aligned} e^+ + e^- &\to \bar{\nu} + \nu \\ \gamma^\star &\to \bar{\nu} + \nu. \end{aligned} \tag{1}$$

After the start of silicon burning, additional neutrino emission processes play an important role: electron capture on nuclei and free protons

$$\begin{aligned} (Z, A) + e^- &\to (Z-1, A) + \nu_e \\ p + e^- &\to n + \nu_e \end{aligned} \tag{2}$$

and β^+ and β^- decays of nuclei:

$$\begin{aligned} (Z, A) &\to (Z-1, A) + e^+ + \nu_e \\ (Z, A) &\to (Z+1, A) + e^- + \bar{\nu}_e \end{aligned} \tag{3}$$

During the final silicon burning phase average energies grow to several MeV and this signal can be detected by neutrino experiments with a sufficiently low energy threshold, if the distance is not too far (up to 1 kpc) several hours before the core collapse.

Core collapse I: Initial phase

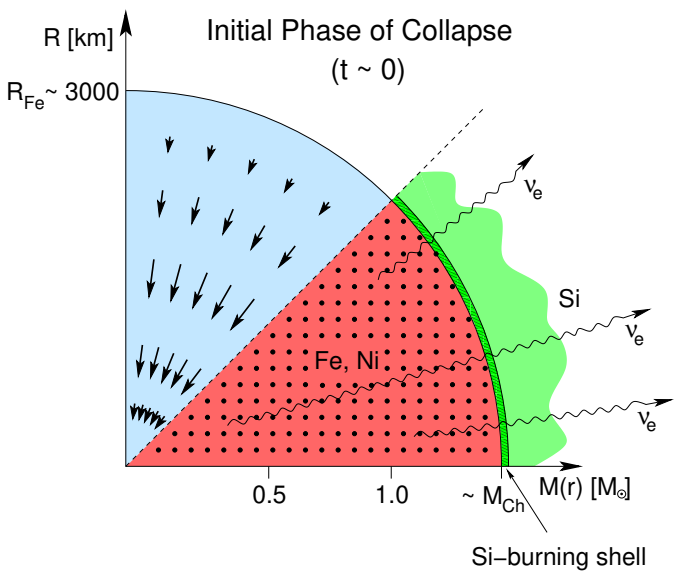

Figure: Figures from H.-Th Janka et al. 2007

The iron core contracts, its density increases.
Thermal energy of the core is decreased by the endothermic reaction of iron photodissociation:

$$^{56}Fe \rightarrow 13\alpha + 4n,$$

and via electron capture:

$$(Z, A) + e^- \rightarrow (Z - 1, A) + \nu_e$$
$$p + e^- \rightarrow n + \nu_e$$

also decreasing electron abundance.
The resulting neutron-rich nuclei are then fused together to form heavier elements, as the core continues its collapse and densities increase.

Core collapse II: Neutrino trapping

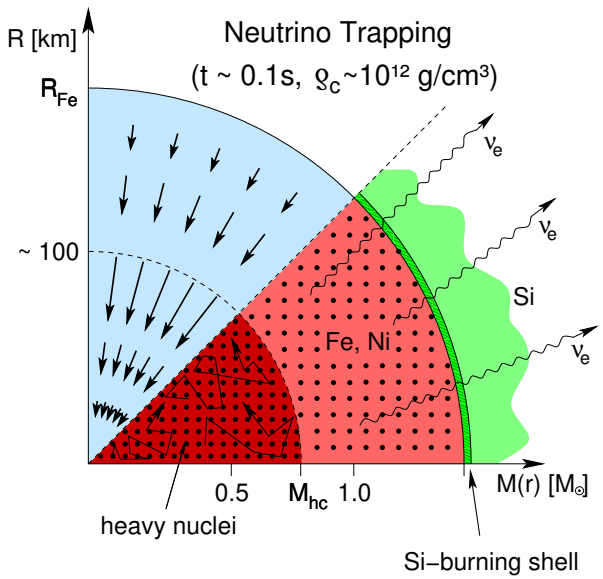

Figure: Figures from

The matter density increases and heavier nuclei are produced.
Coherent elastic nuclear scattering

$$\nu + (Z, A) \rightarrow \nu + (Z, A)$$

become dominant, because $\sigma \sim A^2$.
Thus during the collapse, both the the interaction cross-section σ and the matter density ρ are increasing.

$$\rho_{trap} = 10^{12}\,\mathrm{g/cm^3}$$

the neutrinos can't escape the infalling matter.
Neutrinos scattering inside the inner core are keeping the core in thermodynamical equilibrium

"Neutrinosphere": a spherical layer of radius R_ν where the medium becomes mostly transparent to neutrinos.

Core collapse III: Core bounce

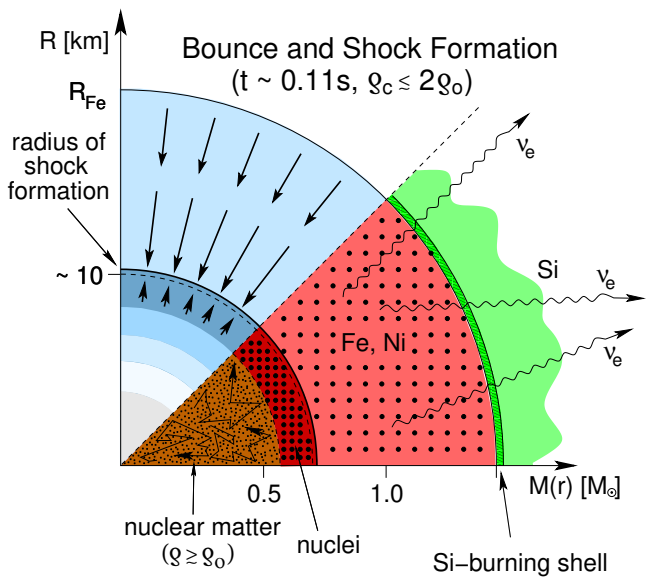

Figure: Figures from

When the density reaches $\rho_0 \sim 10^{14}\,\mathrm{g/cm^3}$ the heavy nuclei form hot dense nuclear matter, which can't be compressed any further because of the strong interaction forces.
This leads to a buildup of the pressure in the core, which repels the infalling matter from the inner core, forming a discontinuity in the pressure and infall velocity.

This discontinuity forms a mild pressure wave, which eventually becomes a shockwave as it expands outwards from the inner core to the less dense shells.
It pushes out the external infalling layers, increasing their pressure and entropy.

Core collapse IV: Shock breakout

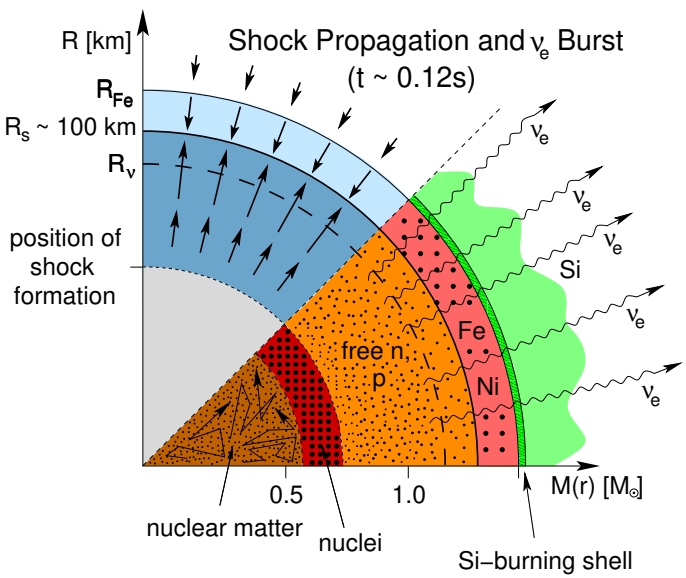

Figure: Figures from

The energy of the shockwave is used up by the photodissociation of the heavy nuclei, so the layers behind the shockwave front consist mostly of free nucleons. Since the electron capture rate on free protons is large, lots of ν_e are produced.

When the shockwave front breaks out beyond R_ν, these ν_e escape the star, carrying away about $10^{51}\,\mathrm{erg}$ within a 10 ms "neutronization peak".

Additionally at this stage the production of $\nu\bar{\nu}$ pairs of all flavors starts to contribute.

Core collapse V: Shock stagnation and revival

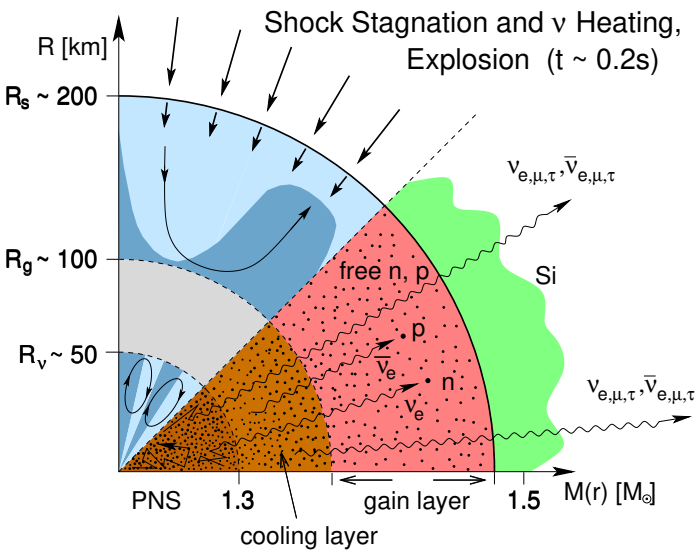

Figure: Figures from

Shockwave stagnates in the outer stellar shells.
The neutrinos produced outside of the neutrinosphere can escape, cooling these layers. These neutrinos interact in the outer layers via charged current interactions

$$\nu_e + n \rightarrow e^- + p$$
$$\bar{\nu_e} + p \rightarrow e^+ + n$$

are reheating the outer "gain" layer, leading to the revival of the stalled shockwave.
This effect suggested is considered to be driving the eventual supernova explosion.

Core collapse VI: Neutrino cooling

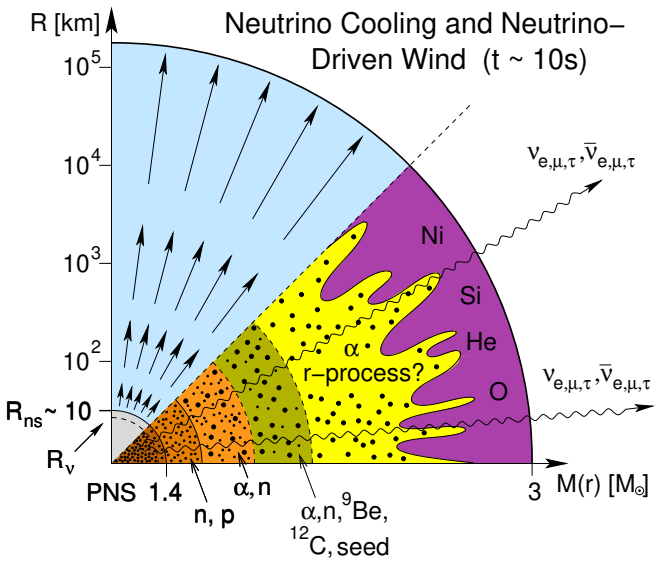

Figure: Figures from

Finally the proto-neutron star is emitting the $\nu\bar{\nu}$ pairs of all flavors equally.
These neutrino can escape freely, cooling the stellar core remnant.

Supernova neutrino signal

Neutrino production and propagation depends on many parameters: progenitor mass, EoS, neutrino mixingand mass ordering.
Neutrino signal can be a probe of these parameters!

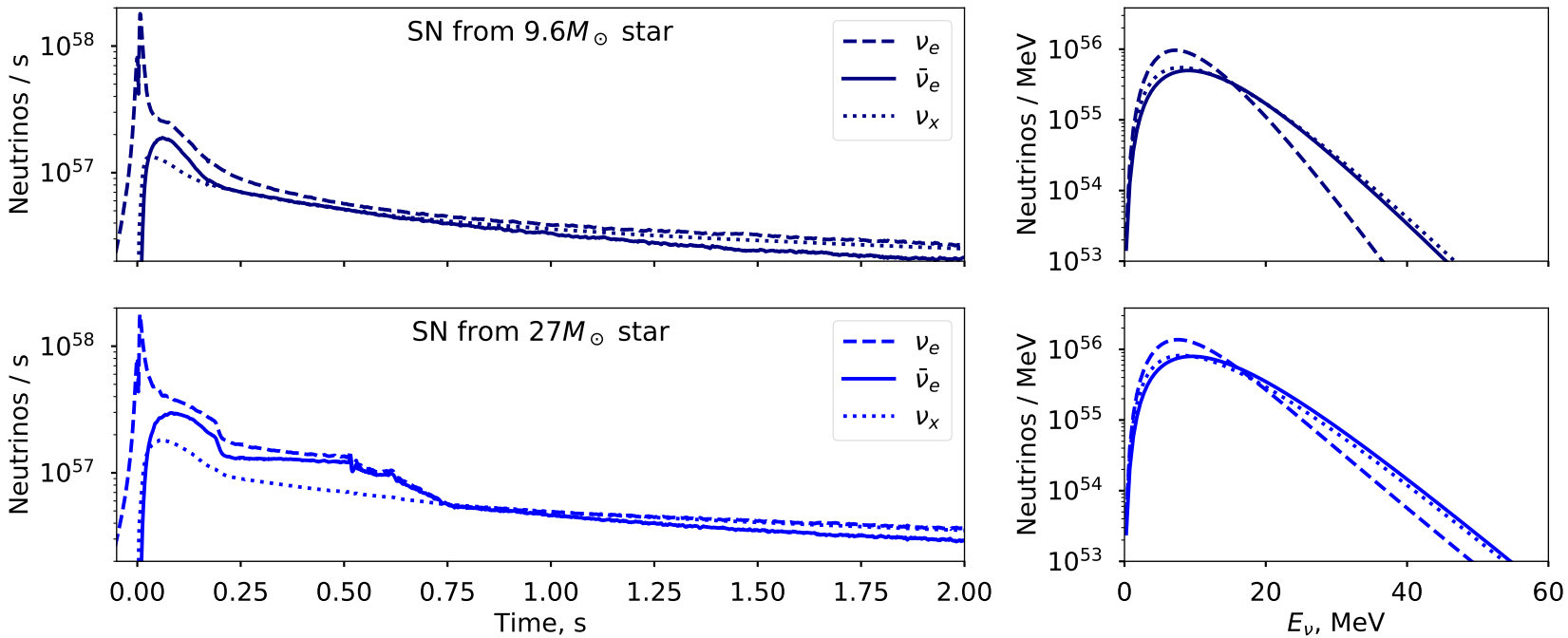

Figure: Expected neutrino production vs. time (left) and energy (right) from collapsing stars with a mass of 9.6 $M_\odot$ (top) and 27 $M_\odot$ (bottom), from the simulation by the Garching group . This simulation does not include flavor changing effects such as neutrino oscillations and collective effects.

Supernova: a multimessenger phenomenon

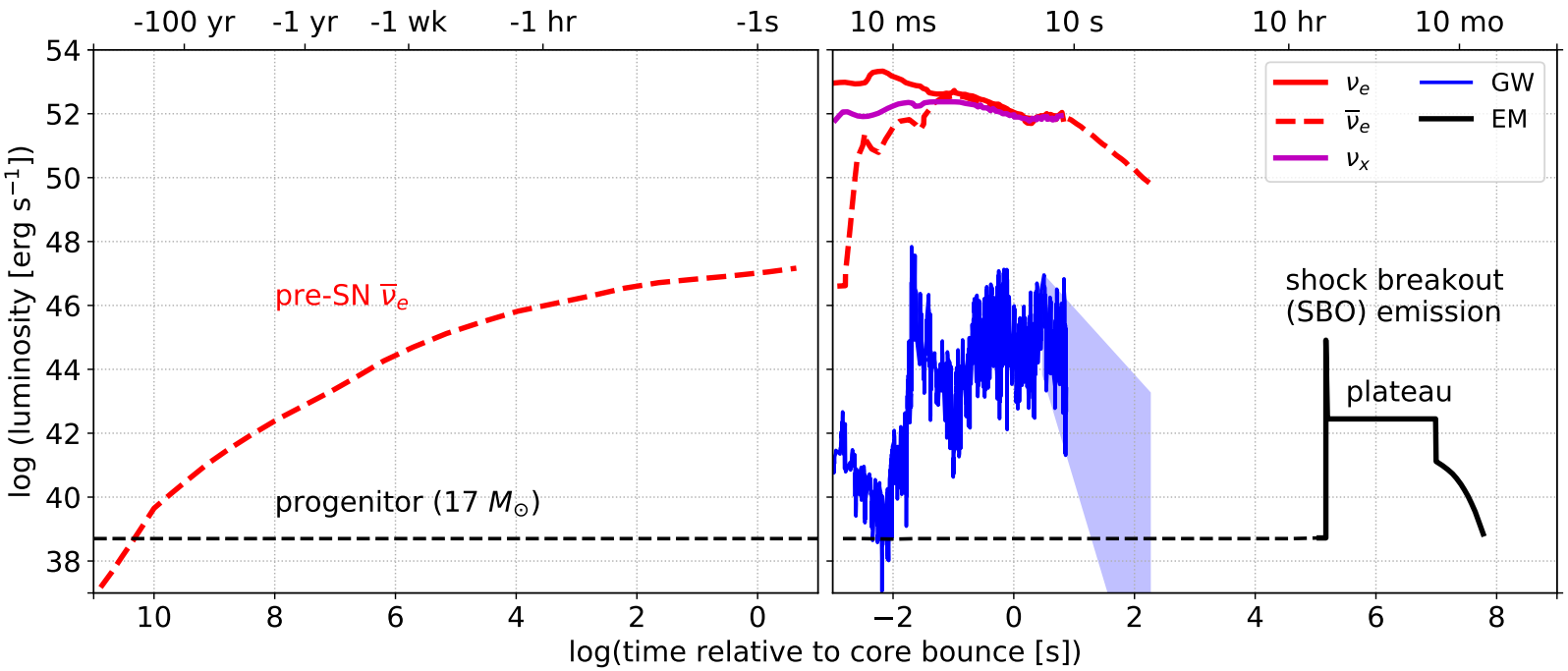

pre-supernova:

- $E_\nu \sim$ 1–10 MeV
- $T \sim$ 10 days

CCSN:

- $N_\nu \sim 10^{58}$ neutrinos
- $E_\nu \sim$ 10–60 MeV
- $T \sim$ 10 s

Neutrinos can serve as an early warning for hours before optical signal

Very rare: 1-3/century in our galaxy.

Detection is a global task: SuperNova Early Warning System

Plan

Detector structure

Main goal of the NOvA experiment: study neutrino oscillations in the muon (anti-)neutrino beam, with $\langle E_\nu \rangle = 2$ GeV.

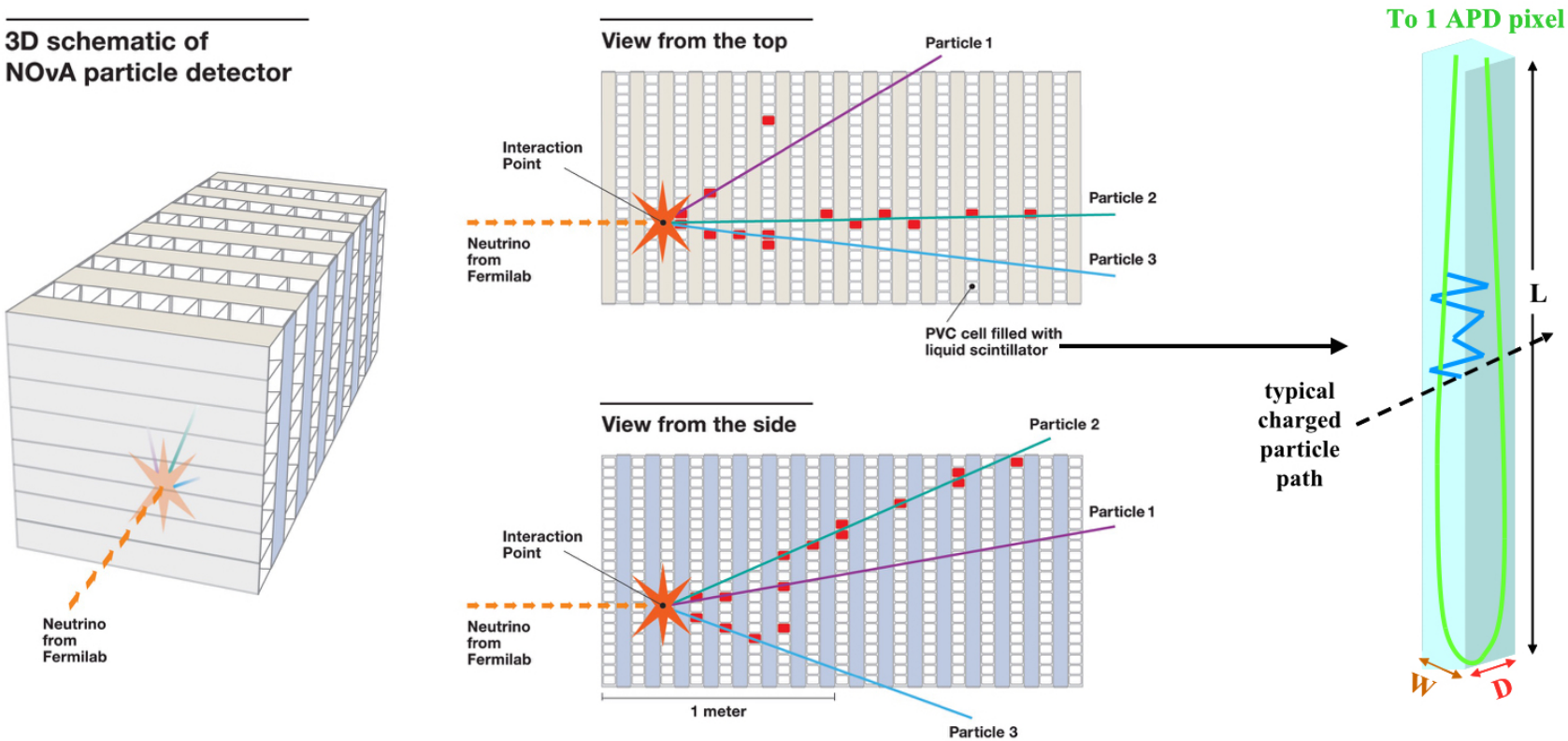

Segmented liquid scintillator detector: PVC cells $6\,\mathrm{cm} \times 4\,\mathrm{cm}$ provide granularity to reconstruct $\sim$ *GeV* neutrino interactions.

NOvA detectors

Two detectors of similar structure, separated by 810 km

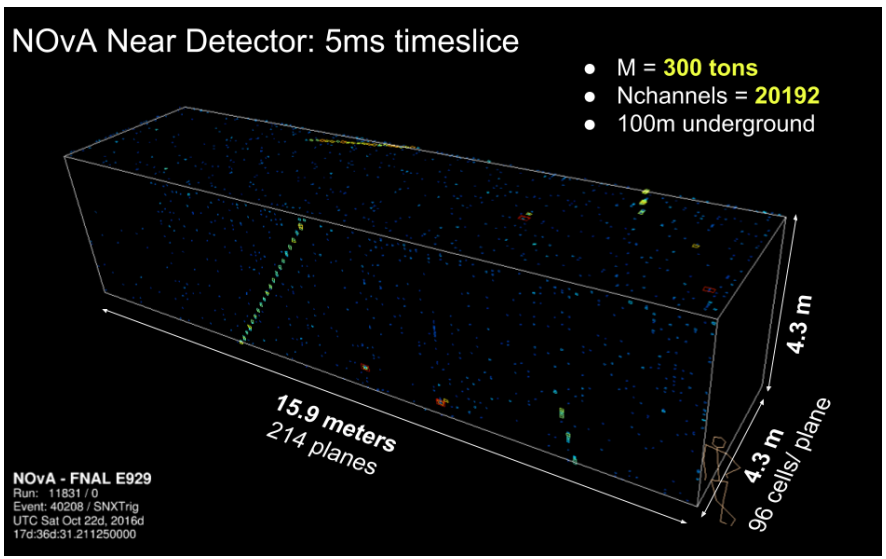

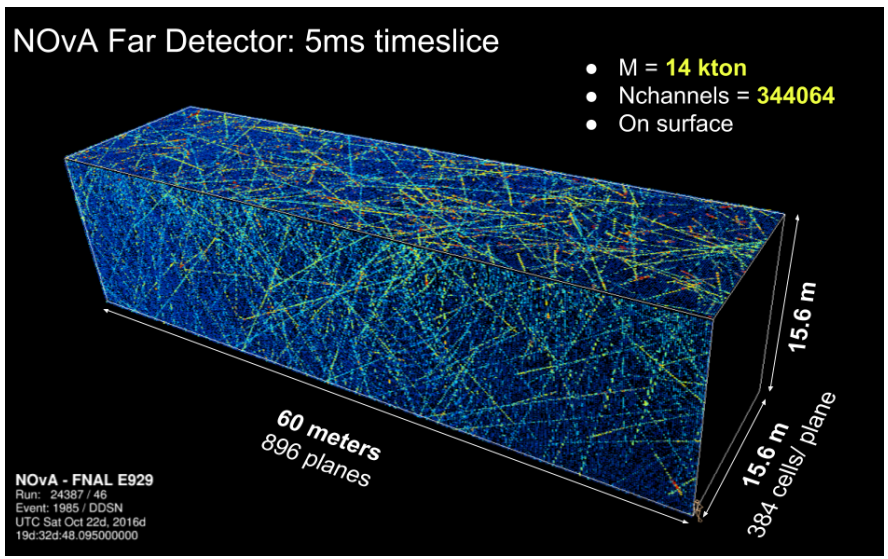

- Similar structure ⇒ almost the same reconstruction and data processing,
- Different size and overburden ⇒ very different BG conditions, statistics.

Low overburden leads to high atmospheric muon activity:
average of 37 Hz in Near Detector and 148 kHz in Far Detector.

NOvA Data Driven Triggers

NOvA has a flexible system of software data driven triggers, to perform additional physics searches:

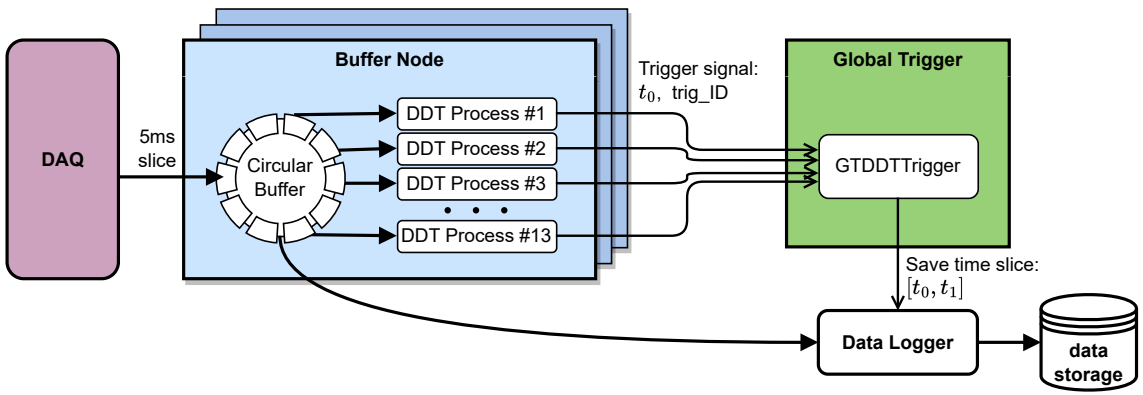

- Data, read from the detector, is sliced in 5 ms chunks (milliblocks)
- Milliblocks are stored in a circular buffer on one of 170(13 for Near Detector) buffer nodes.
- Parallel DDT processes analyze milliblocks, performing fast reconstruction and search for specific signatures.

- If a signal of interest is found — send the time t_0 and `trig_ID` to `Global Trigger` node
- `Global Trigger` which requests the data to be saved in a certain time window around the found signature.
- `Data Logger` reads the requested data from the buffers and saves them for offline analysis.

Buffers can store up to 1350 s (Far Detector) or 1900 s (Near Detector) of data.

Supernova neutrino detection channels

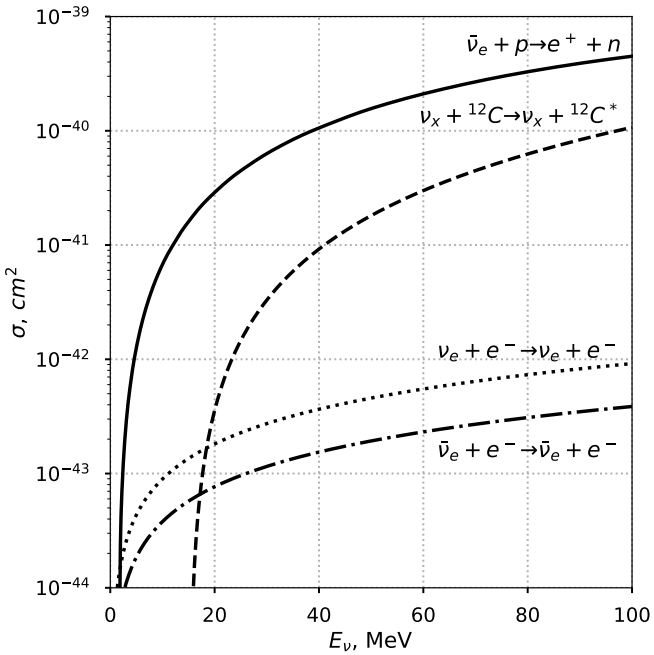

- Inverse beta decay Strumia and Vissani 2003

$$\bar{\nu}_e + p \to e^+ + n$$

- Elastic scattering on electrons Marciano and Parsa 2003

$$\nu_x(\bar{\nu}_x) + e^- \to \nu_x(\bar{\nu}_x) + e^-$$

- NC scattering on carbon Armbruster et al. 1998

$$\nu_x(\bar{\nu}_x) + {}^{12}C \to \nu_x(\bar{\nu}_x) + {}^{12}C^*(15.1\ \text{MeV})$$

Interaction channel	Far Detector		Near Detector	
	$9.6\,\mathrm{M}_\odot$	$27\,\mathrm{M}_\odot$	$9.6\,\mathrm{M}_\odot$	$27\,\mathrm{M}_\odot$
Inverse beta decay	1593	3439	24	51
Elastic scattering on e^-	143	259	3	5
Neutral current on $^{12}\mathrm{C}$	67	166	1	3
Total	1803	3864	28	59

Signal sample

Simulation of SN neutrino interactions in Far Detector using GenieSNova package (developed for this work)

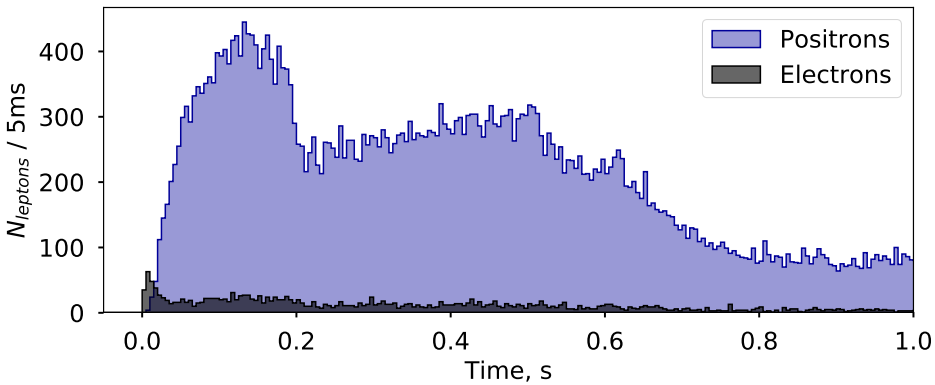

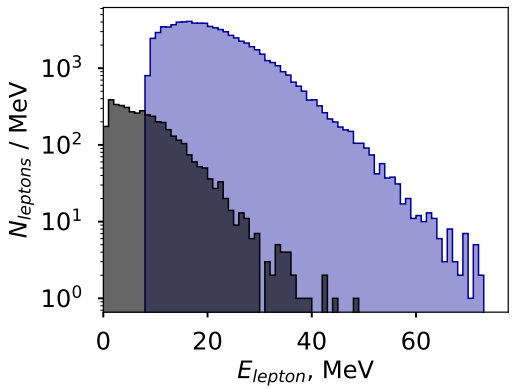

Signal is very faint compared to background!

- IBD positron from SN neutrino produces 1–5 *hits* — signals in nearby PVC cells.
- Atmospheric muon produces around 400 hits!

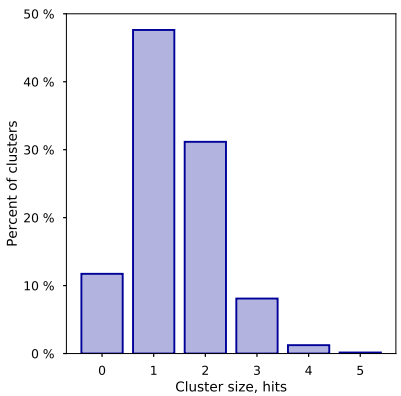

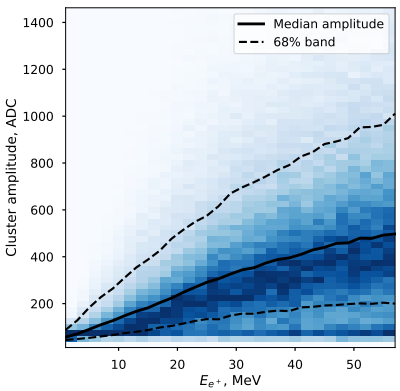

Task

Tag hits from all known background sources; select SN neutrino interactions

Atmospheric muons

Huge amount of atmospheric muons in Far Detector. Michel electrons have $E_e \leqslant 53\,\mathrm{MeV}$ and can mimic IBD positron response.

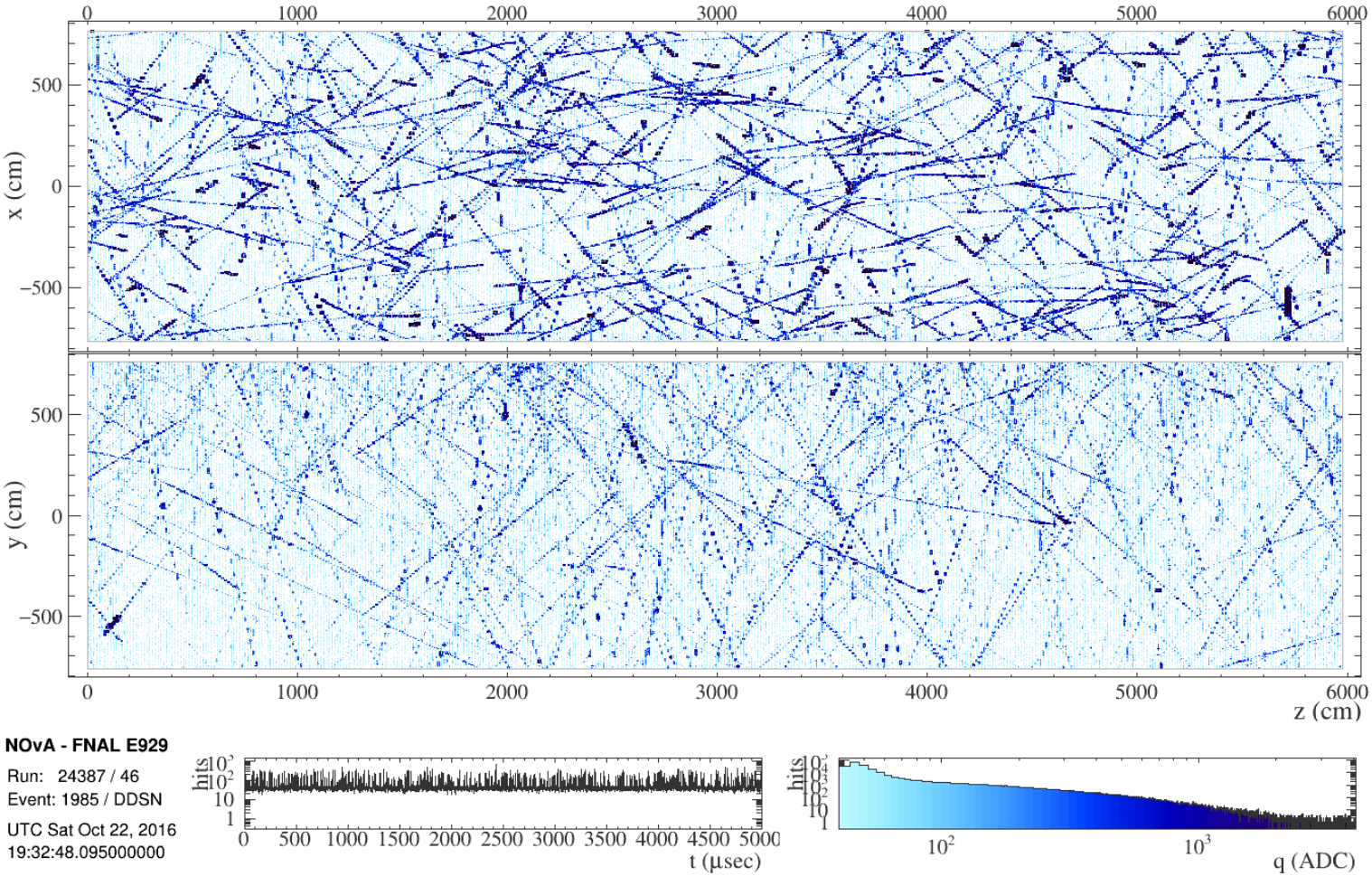

Tag: find the muon tracks using Hough transform; tag all hits around the track as *muons*; tag all hits around track endpoint within 10 μs and 32 cm as *Michel electrons*

High energy showers

High energy atmoshperic showers hit the Far Detector several times per hour. The excited nuclei produce delayed activity after the shower.

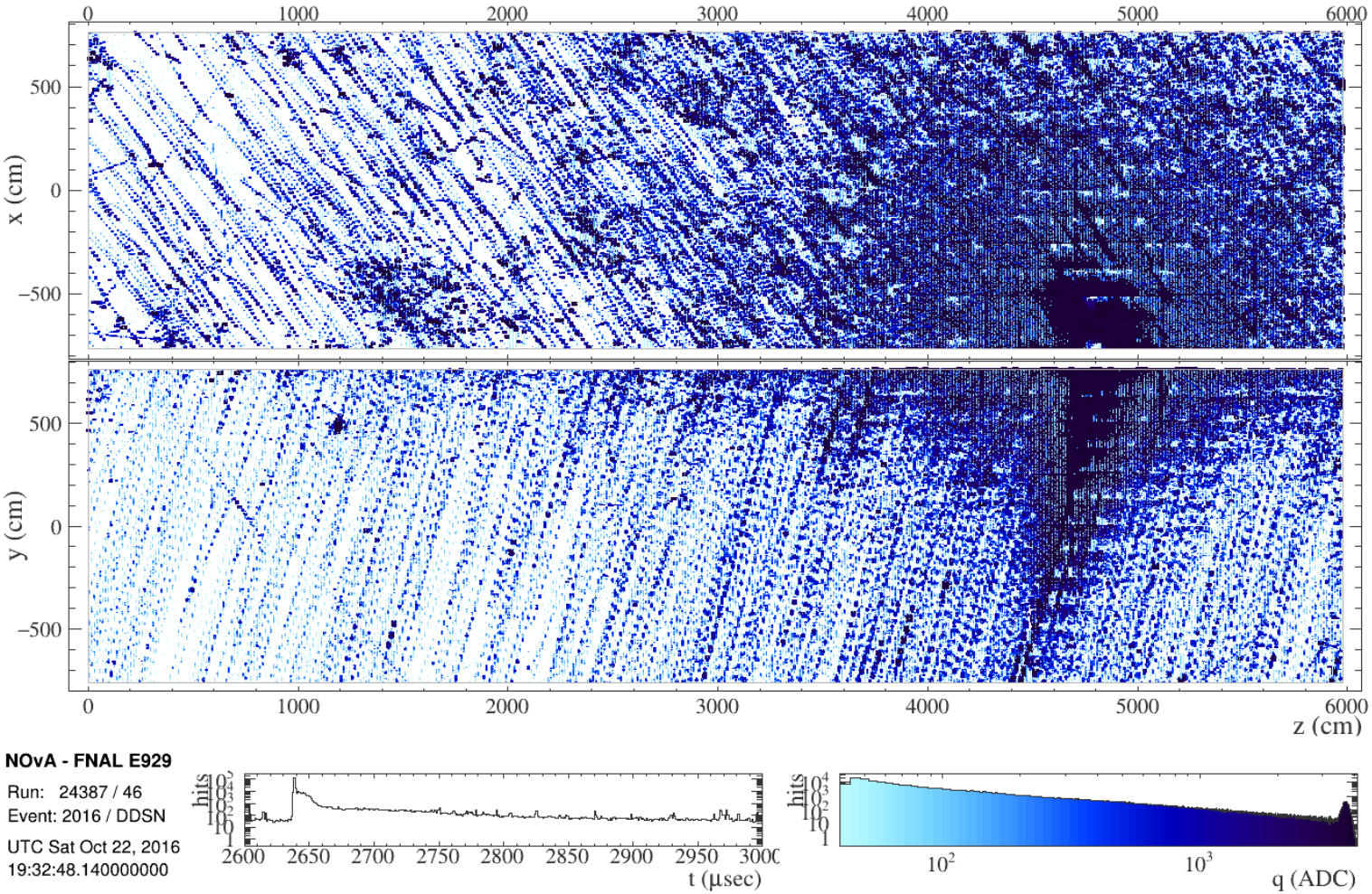

Tag: find the time t_0 of the peak amplitude, tag all hits within 350 μs window after t_0

Electronic channel noise

Front-end readout electronics failures can lead to excessive/suppressed hit rates in individual channels or in groups of 32 neighbouring channels.
A special service is monitoring activity in each channel, and creates a map of tagged channels every 1 hour

- "cold" channels: inactive 90% of time
- "hot" channels: 1 hour averaged activity above 1 kHz
- "mixed" channels: acting both as cold and hot within 1 hour

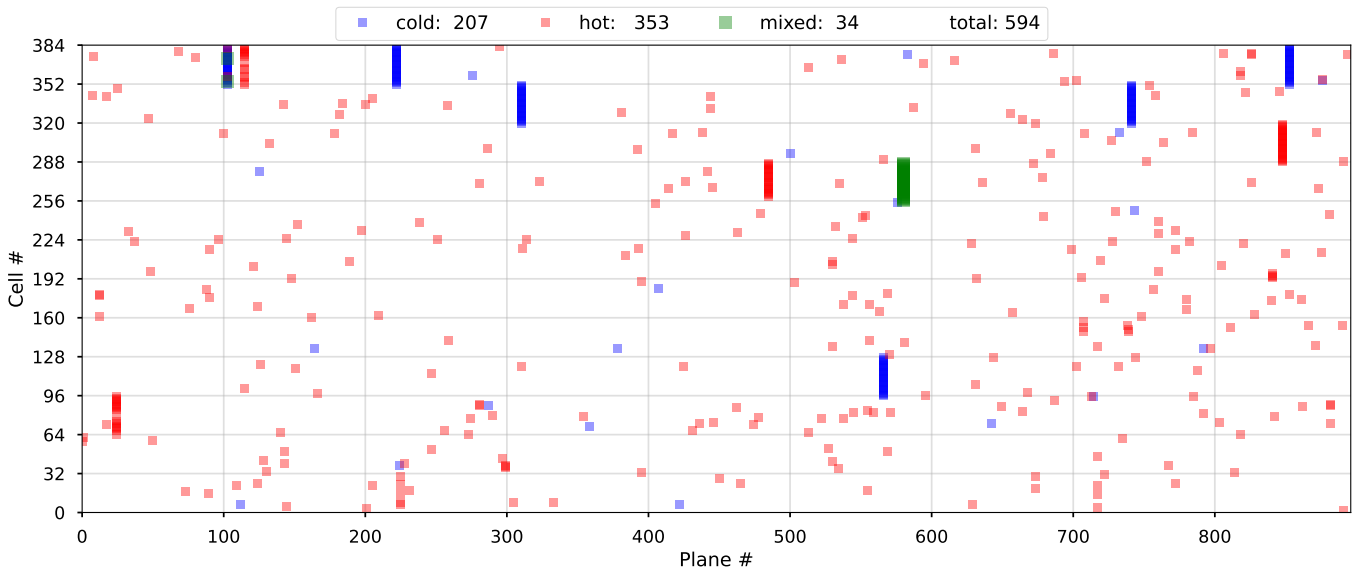

Tag: all the hits from the channel if it was hot/cold within last 24 hours.

Electronic channel noise

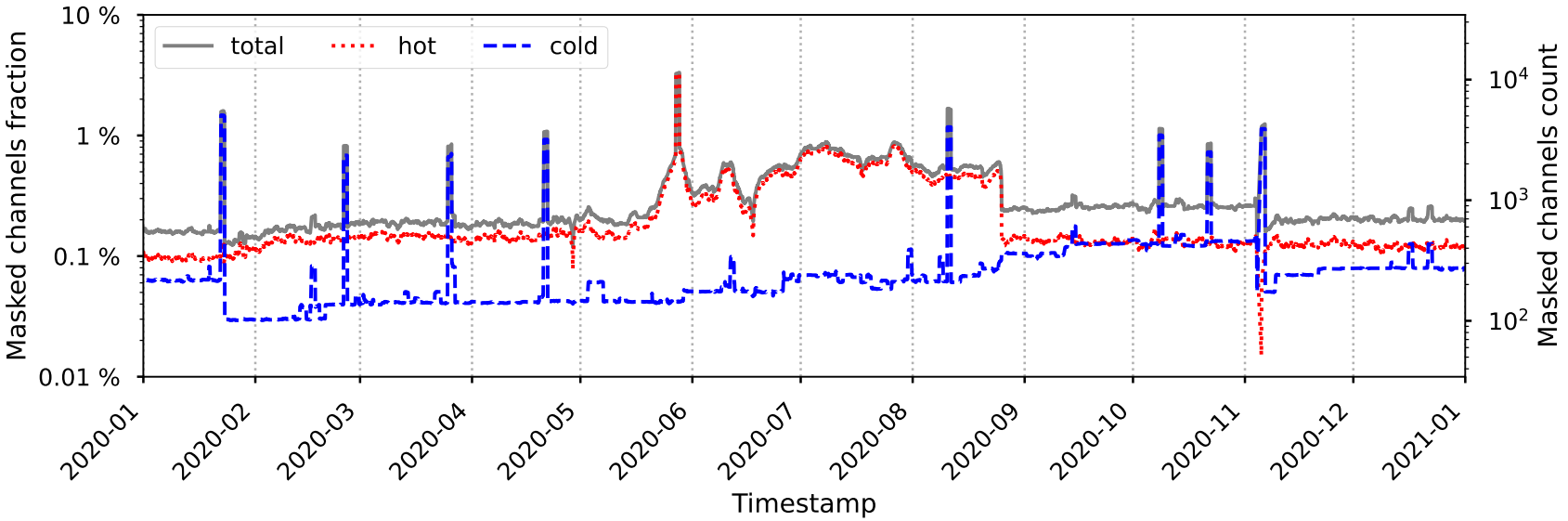

Figure: Fraction of readout channels excluded from the Far Detector supernova analysis vs. time during the year 2020. One can see the rise of "hot" channels amount during summer period, ending with the stabilisation at the end of the detector maintenence work. The spikes in the "cold" channels fraction plot correspond to the malfunction of the electronic modules, which group the readout of many channels. These modules are restored by an automatic reboot or repaired during maintenance.

Background suppression results

		Average hit rate, kHz	Fraction	Variation
Far Detector	Total detector hit rate	74971.09	100.00%	1.21%
	Hits from cosmic ray muons	16702.19	22.28%	5.06%
	Hits from Michel electrons	4727.62	6.31%	5.18%
	Single channel noise	1533.98	2.05%	2.04%
	High energy shower activity	96.26	0.13%	839.35%
	Activity after selection	56344.94	75.16%	0.89%
Near Detector	Total detector hit rate	715.14	100.00%	11.01%
	Hits from cosmic ray muons	2.57	0.36%	255.36%
	Hits from Michel electrons	1.14	0.16%	295.76%
	Single channel noise	445.88	61.90%	10.60%
	High energy shower activity	0.04	0.01%	8796.71%
	Activity after selection	269.89	37.74%	9.03%

Clustering algorithm

In order to find the group of hits produced by a single neutrino interaction, a clustering in time and space is applied.
Hits belong to the same cluster if they are in:

- the same plane and separated by not more than 1 cell (hits 1+2, or 3+4);
- adjascent planes (hits 3+5, 4+5).

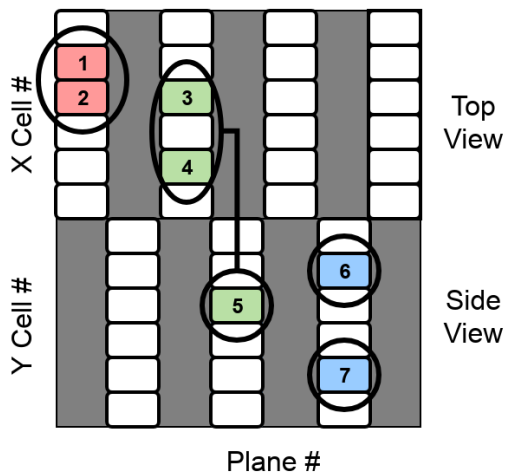

- Have time difference $\Delta t \leqslant 32\,\mathrm{ns}$

The time precision of a single observed hit is 8–12 ns depending on its amplitude.

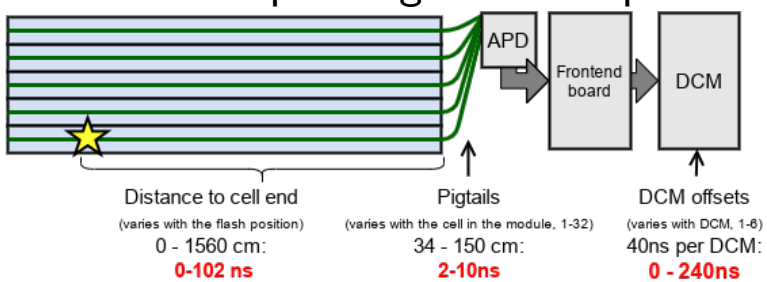

However the time of the initial scintillation flash is delayed in the readout system by up to 240 ns, which needs to be taken into account.

Signal: small clusters $N_{hits} \leqslant 4$ in both X and Y view
Background: large clusters $N_{hits} > 4$ (physics background events), or small clusters in the same view (correlated electronic noise)

Candidate selection: ADC

We find optimal ADC cuts by optimizing $S/\sqrt{B}$ for $9.6\,\mathrm{M}_\odot$ model at the 10 kpc distance:

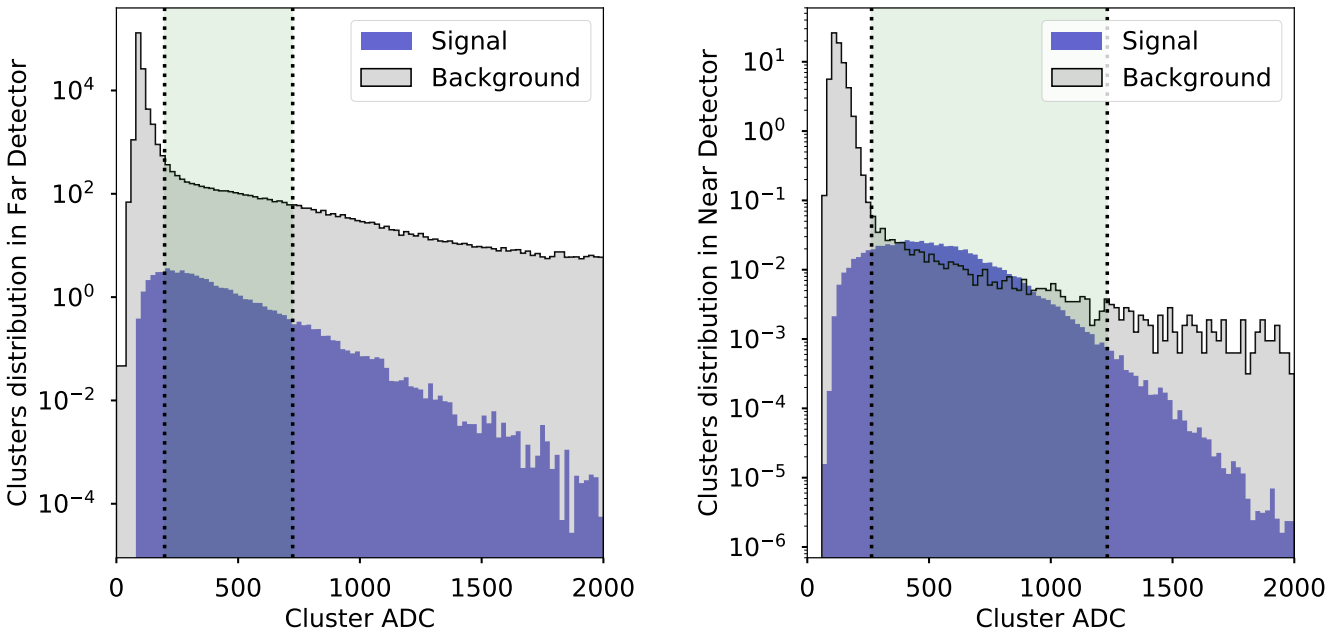

And remove candidates close to the detectors' borders, to reduce external background:

Cut	Near Detector	Far Detector
ADC range	[280, 1430]	[230, 910]
Fiducial volume	$8 \leqslant$ X cell $\leqslant 88$ $8 \leqslant$ Y cell $\leqslant 88$ $8 \leqslant$ Z plane $\leqslant 184$	$16 \leqslant$ X cell $\leqslant 368$ $16 \leqslant$ Y cell $\leqslant 360$ $8 \leqslant$ Z plane $\leqslant 888$

Removing time-correlated groups

Signal candidates should be uncorrelated on short timescales.
Background candidates produced by the atmospheric events, atmospheric showers etc. produce groups of candidates at the same time.

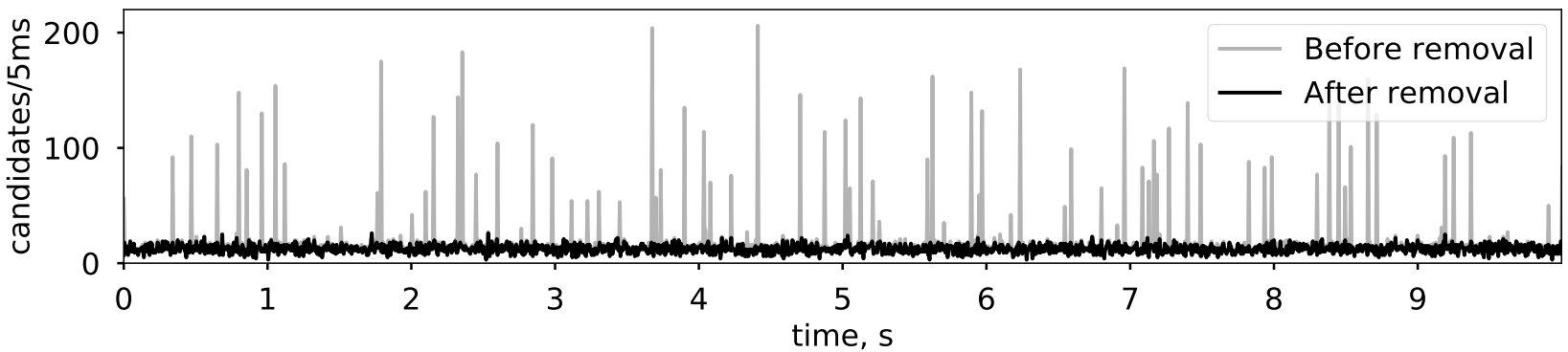

We reject any pair of interaction candidates with timestamps closer than 250 ns.
This rejection produces a dead time less than 0.15%.
This significantly decreases the variation of the background candidates in time so that the background level follows a Poisson distribution.

Selection results

	Cut	Background		Signal	
		N_{bg}/s	ε	N_{sg}/s	ε
Far Detector	Reconstructed clusters	322811.99	100.00%	316.24	100.00%
	X and Y hits	231866.53	71.83%	145.16	45.90%
	$N_{hits} \leqslant 4$	310010.78	96.03%	315.06	99.63%
	Fiducial Volume	172281.67	53.37%	118.45	37.46%
	ADC cut	25879.67	8.02%	216.38	68.42%
	Total	**2483.21**	**0.77%**	**86.64**	**27.40%**
Near Detector	Reconstructed clusters	403.95	100.00%	3.16	100.00%
	X and Y hits	215.64	53.38%	2.19	69.35%
	$N_{hits} \leqslant 4$	394.81	97.74%	3.15	99.67%
	Fiducial Volume	68.10	16.86%	1.49	47.23%
	ADC cut	24.30	6.02%	2.73	86.29%
	Total	**0.52**	**0.13%**	**1.28**	**40.43%**

The signal events correspond to the first second of a 9.6 $M_\odot$ model at 10 kpc distance.

Selection results

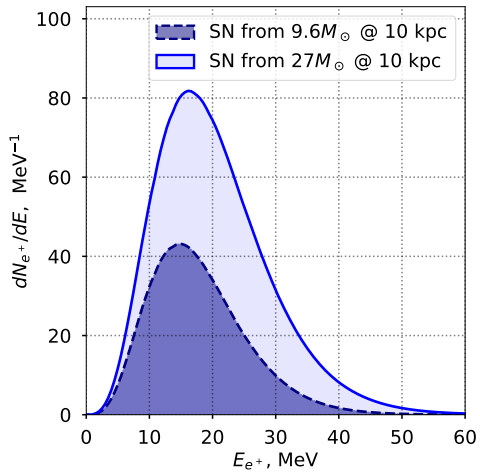

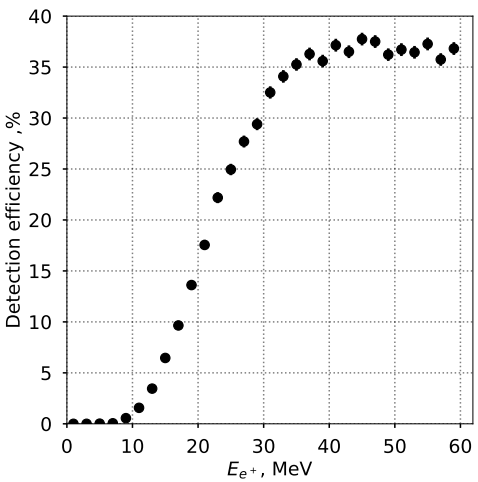

The background suppression, reconstruction and selection of neutrino interaction candidates allowed to reduce background rate

- Far Detector: from about 75×10^6 hits/s to 2500 cands/s
- Near Detector: from about 7×10^5 hits/s to 0.52 cands/s

Remaining signals:

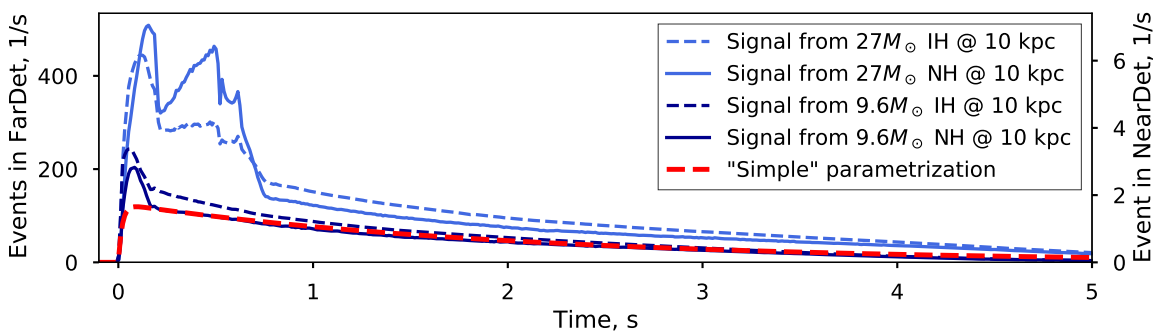

Plan

Goal of statistical analysis

Input data from the candidates selection: time series

$$n_i = b_i + s_i$$

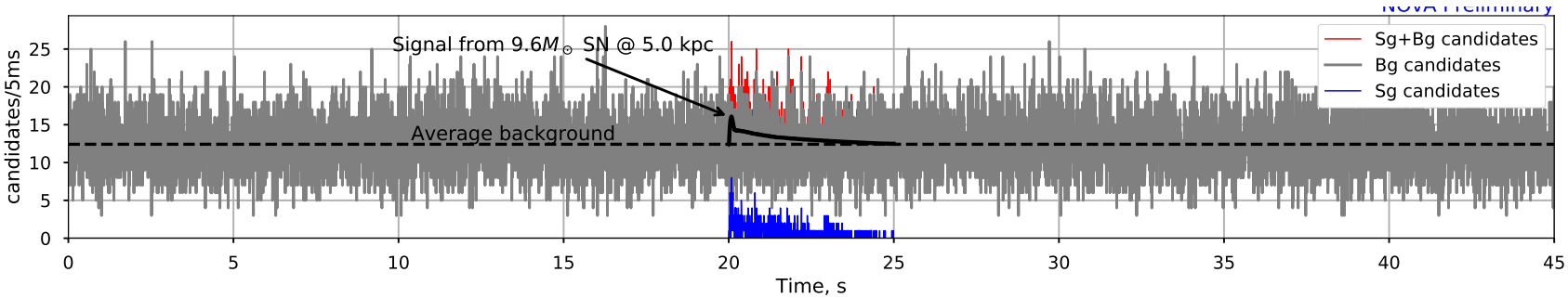

Task

- determine the presence of a SN signal the data $\{t_i\}$,
- determine the starting time t^* and the significance z of this signal.

As this is method for low-latency processing:

- Robust and simple calculations of signal significance
- Avoid scanning through all the signal parameters (models, progenitor mass, distance, neutrino mass ordering)
- Scan the signal starting time t^* parameter

Hypothesis test

The triggering system needs to distinguish between the "background only" H_0 and "background+signal" H_1 hypotheses, using data $\vec{n} = \{n_i\}$.

- In general: a **test statistic** function $\ell(\vec{n})$ to discriminate H_0 vs. H_1.
- The signal significance is characterized by p-value:

$$p(\ell) = \int_{\ell}^{\infty} P(\ell'|H_0)\, d\ell'$$

- For convenience this can be converted to a z-score: $z(\ell) = \Phi^{-1}(1 - p(\ell))$, where $\Phi(x)$ — cumulative standard normal distribution.

Note

z-score is equivalent to that derived in Gaussian statistics as the number of sigma away from the mean

Trigger fires if significance exceeds threshold (whatever definition we use):

$$\alpha = 1/week \iff p_{thr} = 8.267 \cdot 10^{-9}/5ms \iff z_{thr} = 5.645\sigma$$

Counting Analysis (CA)

Common approach for SN detection: count the number of events n in a time window $[t^*, t^* + \Delta t]$:

$$\ell_{CA}(t^*, \Delta t, \{t_i\}) = n \equiv \sum_i w\left(t_i - t^*, \Delta t\right),$$

where $w(t, \Delta t)$ is a window function

$$w(t, \Delta t) = \begin{cases} 1, & t \in [0, \Delta t], \\ 0, & \text{otherwise.} \end{cases}$$

Advantages:

- Simple and robust
- Independent of signal models
- $P(\ell_{CA}|H_0)$ is Poisson distribution around expected background

Disadvantages:

- Maximal ℓ_{CA} around signal maximum, not starting
- Low time precision (defined by Δt)
- Optimal Δt defined by optimizing $S/\sqrt{B}$, so need several windows for distance/models/detector conditions
- Suboptimal for high background case

Shape Analysis (SA)

It's possible to maximize the discrimination for a specific signal model by using the log likelihood ratio:

$$\ell_{SA}(t^*, \{t_i\}) = \log \frac{P(\{t_i\}|H_1)}{P(\{t_i\}|H_0)} = \sum_i \log\left(1 + \frac{S(t_i - t^*)}{B(t_i)}\right),$$

where $B(t)$ is the background event rate, and $S(t)$ is the expected signal event rate over time, relative to supernova start time t^*.

If events are grouped in time bins with edges $\{T_i\}$ and number of events $\{n_k\}$, ℓ is a sum over time bins:

$$\ell_{SA}(t^*, \{n_k\}) = \sum_k n_k \cdot \log\left(1 + \frac{S(T_k - t^*)}{B(T_k)}\right)$$

Note

SA approach is equivalent to CA if the expected signal shape is chosen to be a constant within a counting window: $S(t) \sim w(t, \Delta t)$.

Test statistic distribution

Say we have observed n events with timestamps $\{t_i\}$ within time window Δt.
Hypothesis H predicts event rate $r(t)$, and total rate in window R

We need to know $P(\ell|H)$ in order to calculate significance.

Test statistics in CA and SA are additive functions of data: $\{t_i\}$: $\ell(\{t_i\}) = \sum_i \ell(t_i)$.

It allows us to express $P(\ell|H)$ as an inverse Fourier transform via the characteristic function of single event $\Phi(z) = \mathcal{F}\{P(\ell|1, H)\}$ and predicted total rate R:

$$P(\ell|H) = \mathcal{F}^{-1}\left\{e^{R[\Phi(z)-1]}\right\}$$

$\Phi(z)$ can be computed numerically.

Combining experiments

In case of multiple experiments each using their own test statistic functions $\{\ell_n(t)\}$, their combination is nontrivial.
But for the case of SA, LLRs are additive, and we can define a joint test statistic

$$\ell_{comb} = \sum_{n=1}^{N_{exp}} \ell_n(\{t_i^n\}) = \sum_{n=1}^{N_{exp}} \sum_i \ell_n(t_i^n),$$

Each experiment has its Φ_n and R_n, so the ℓ_{comb} distribution is

$$P(\ell_{comb}|H) = \mathcal{F}^{-1} \left\{ \prod_{n=1}^{N_{exp}} \exp\left(R_n[\Phi_n(z) - 1]\right) \right\}.$$

Example

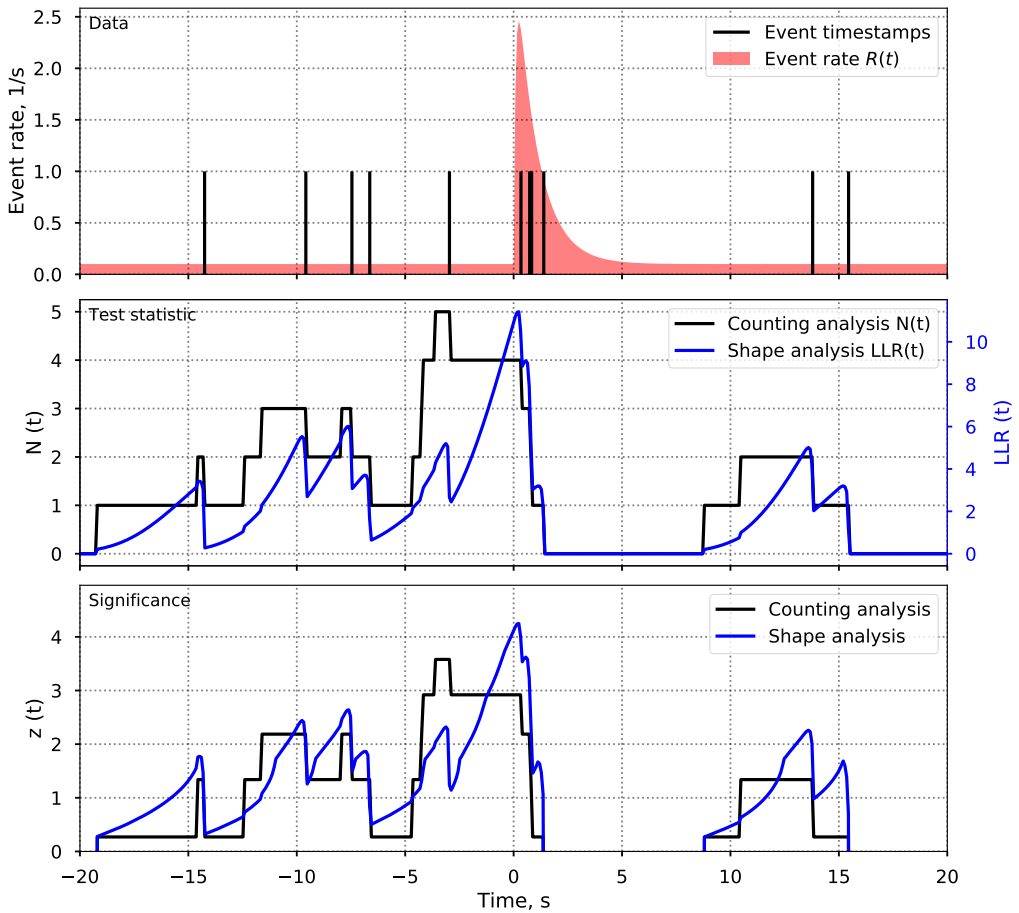

Preparation steps:

1. Define the $B(t)$ and $S(t)$.
2. Compute the single event distribution $P(\ell|1, H_0)$, and its Fourier image $\Phi(z)$.
3. Calculate the test statistic distribution $P(\ell|H_0)$.

For each assumed SN starting time t^*:

1. Calculate $\ell(t^*, \{t_i\})$
2. Evaluate the significance z using $P(\ell|H_0)$

Implemented as python package: Andrey Sheshukov 2021

Note

SA is more complicated than CA. But preparation steps should only be done when B changes; in NOvA: every 10 min.

Plan

Scheme of SN detection system

An extension of usual DDT processing infrastructure.

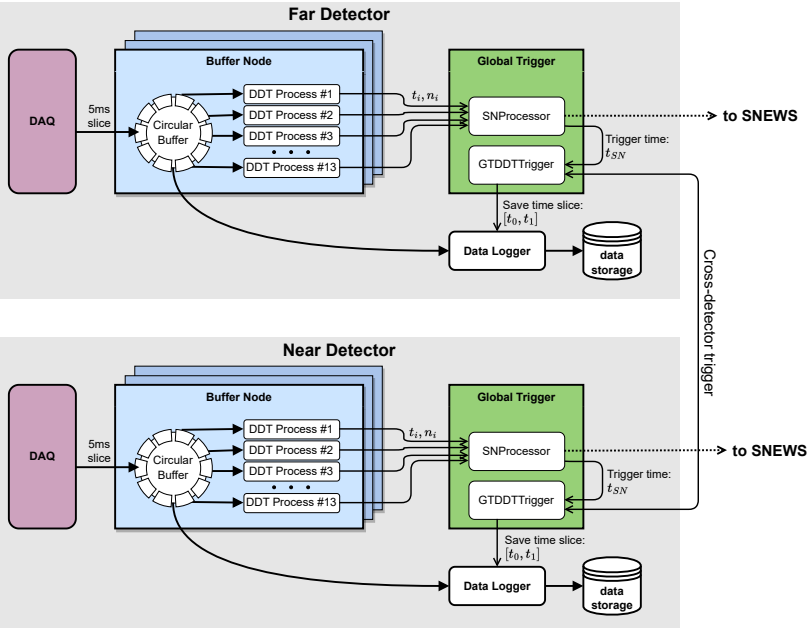

Modules in each of `DDT Processes` perform:

- Monitoring the channels activity to update noisy channels mask every hour (one process per detector).
- Background tagging, clustering, candidates selection as described in section 2
- Sending resulting number of candidates n_i per 5 μs to ZMQ socket.

`SN Processor` module receives the neutrino candidates rate n_i and performs

- Buffering, filtering (removing unstable data)
- Calculation of the SN significance using Shape Analysis
- Identification of the SN signal starting time t^*.

When the SN significance exceeds threshold, sending signal to

- Data Logger to save the 45 s of data around t^*.
- Another detector, to save the data
- SNEWS server to provide other experiments with early warning

Main design goal of the system: flexibility, sustainability, minimal latency

Latency

Supernova neutrino triggering system in NOvA

The system needs to be low latency to act as early warning] Approximate latency for processing each 5 μs milliblock on Far Detector

Processing step	Where	Δt,s
Readout and write to buffer	DAQ	3.5
Reconstruction and selection	DDT	5
Accumulate ten milliblocks	DDT	8.5
Accumulate 1 s continuous data	GT	18
Analyze 5 s of data	GT	5

Processing and waiting delays are almost negligible for Near Detector. Maximal delay (timeout) 60 s is reached when some data is lost.

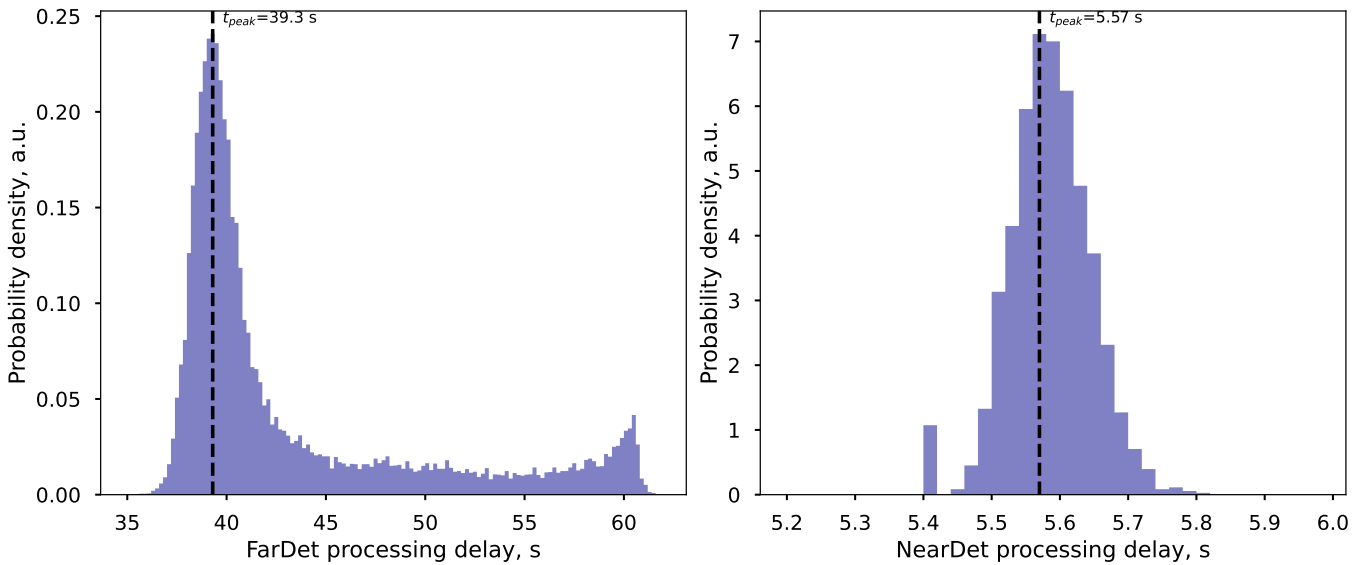

Latency in SNEWS

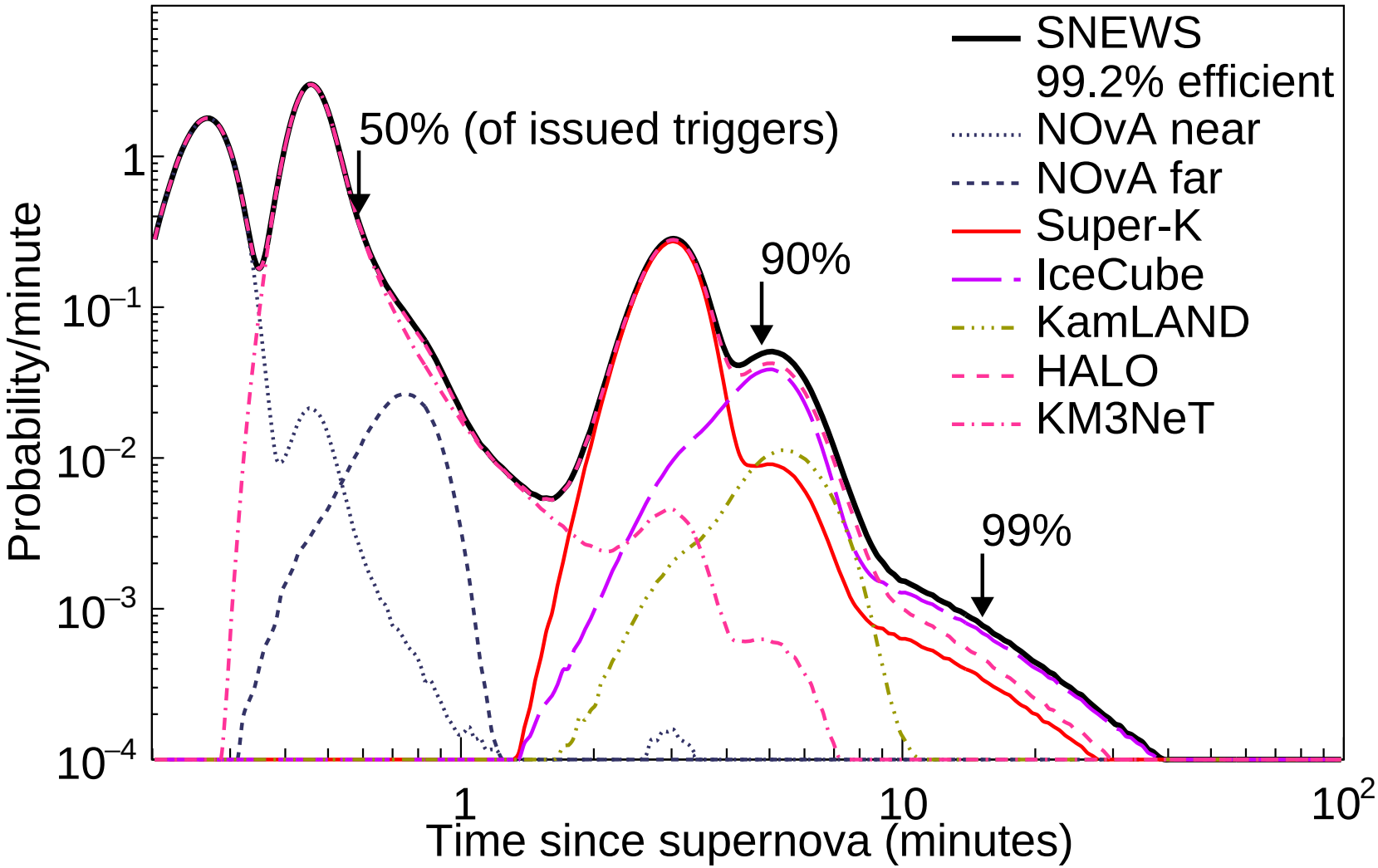

NOvA is now a member of SNEWS with one of the lowest trigger latencies.

Commissioning

Supernova neutrino triggering system in NOvA

During the 318 day commissioning period from October 1, 2018 to August 15, 2019, the NOvA Far Detector triggering system issued **71** supernova triggers.

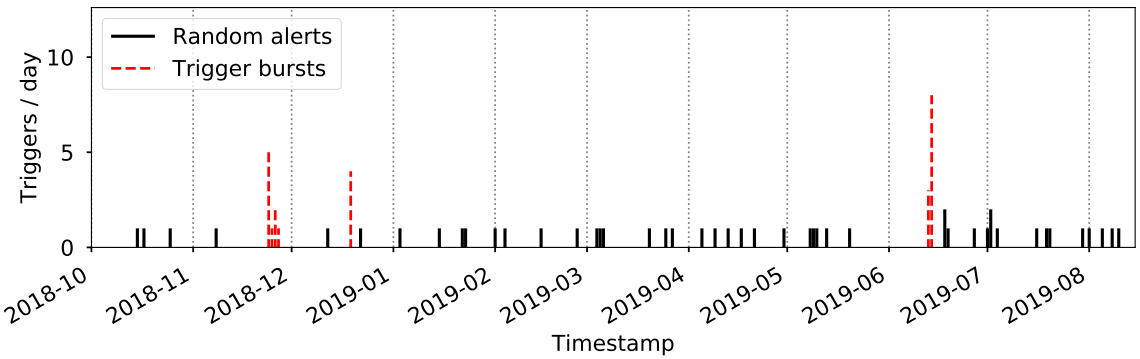

24 triggers concentrated in three bursts, caused by:

- **Partial detector data**
  about 10 min synchronization failure after run restart.
  Solution: Filter incomplete data from the analysis
- **Noise channel map updates failure**
  Solution: additional monitoring of the channel map updating process.

Remaining **47** triggers have average rate $1/(6.77 \pm 0.98\,\mathrm{days})$

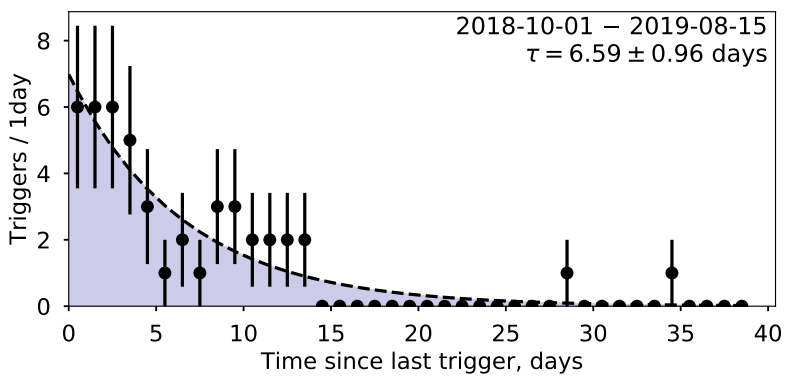

Consistent with design goal $1/7\,\mathrm{days}$

Summary

- A supernova detection system based on NOvA detector data was created and launched, based on the developed reconstruction and selection procedures and statistical processing method.
- The system has a maximal latency of 60 s
- The system has been running on the detectors since November 1, 2017. The triggering events of the system have been studied and are in line with the expected false alarm rate due to statistical background fluctuations.
- The NOvA experiment is a full member of the network and is capable of sending supernova alerts to the SNEWS network. The existing infrastructure is optimized for future modifications that will be required in the development of SNEWSv2.0.
- The low latency of the NOvA supernova triggering system reduces the overall latency of SNEWS network for detecting the supernova signal.

Results published in Acero et al. 2020; Kharusi et al. 2021

Plan

Example of SN signal detection

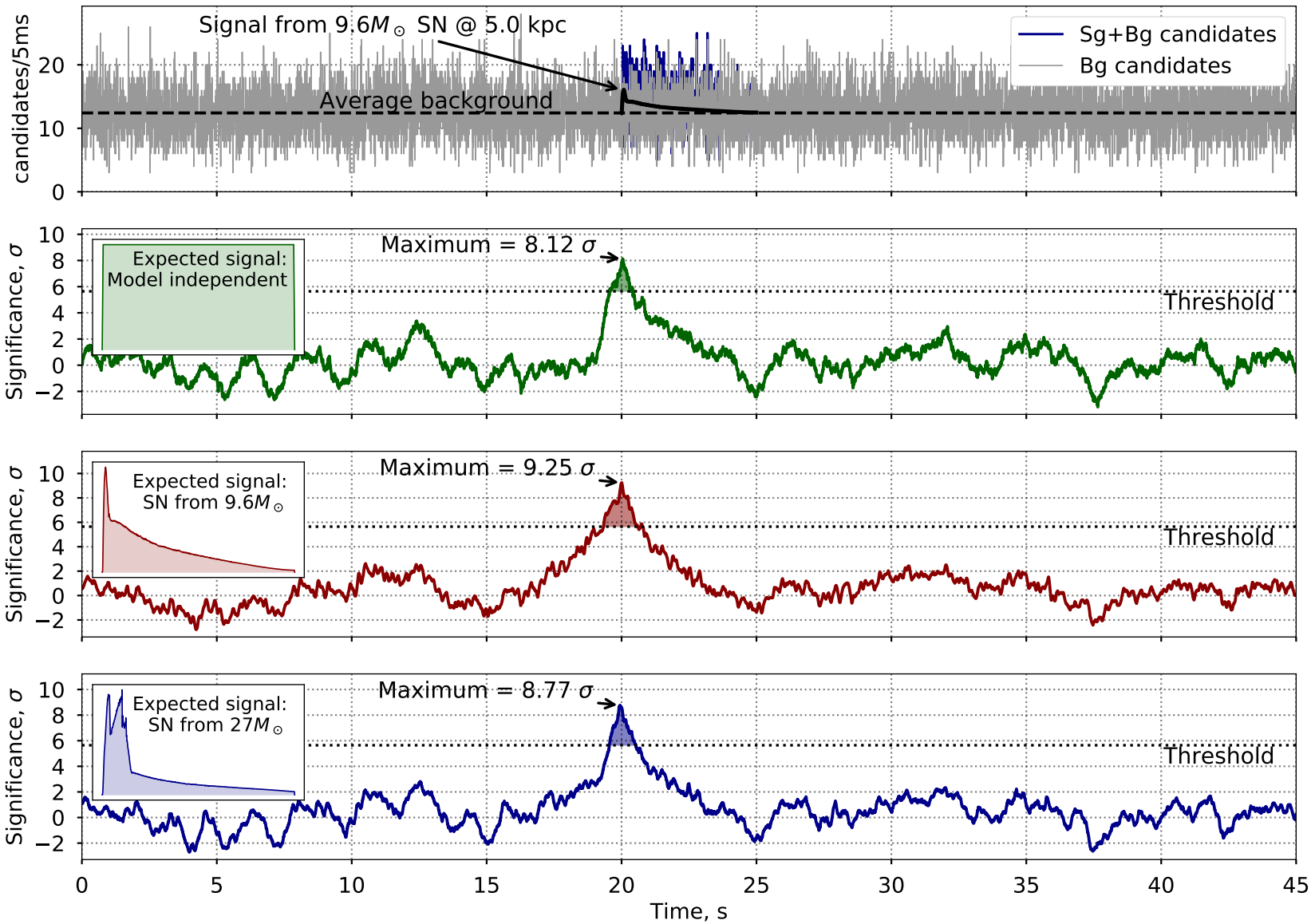

Significance vs. distance in NOvA detectors

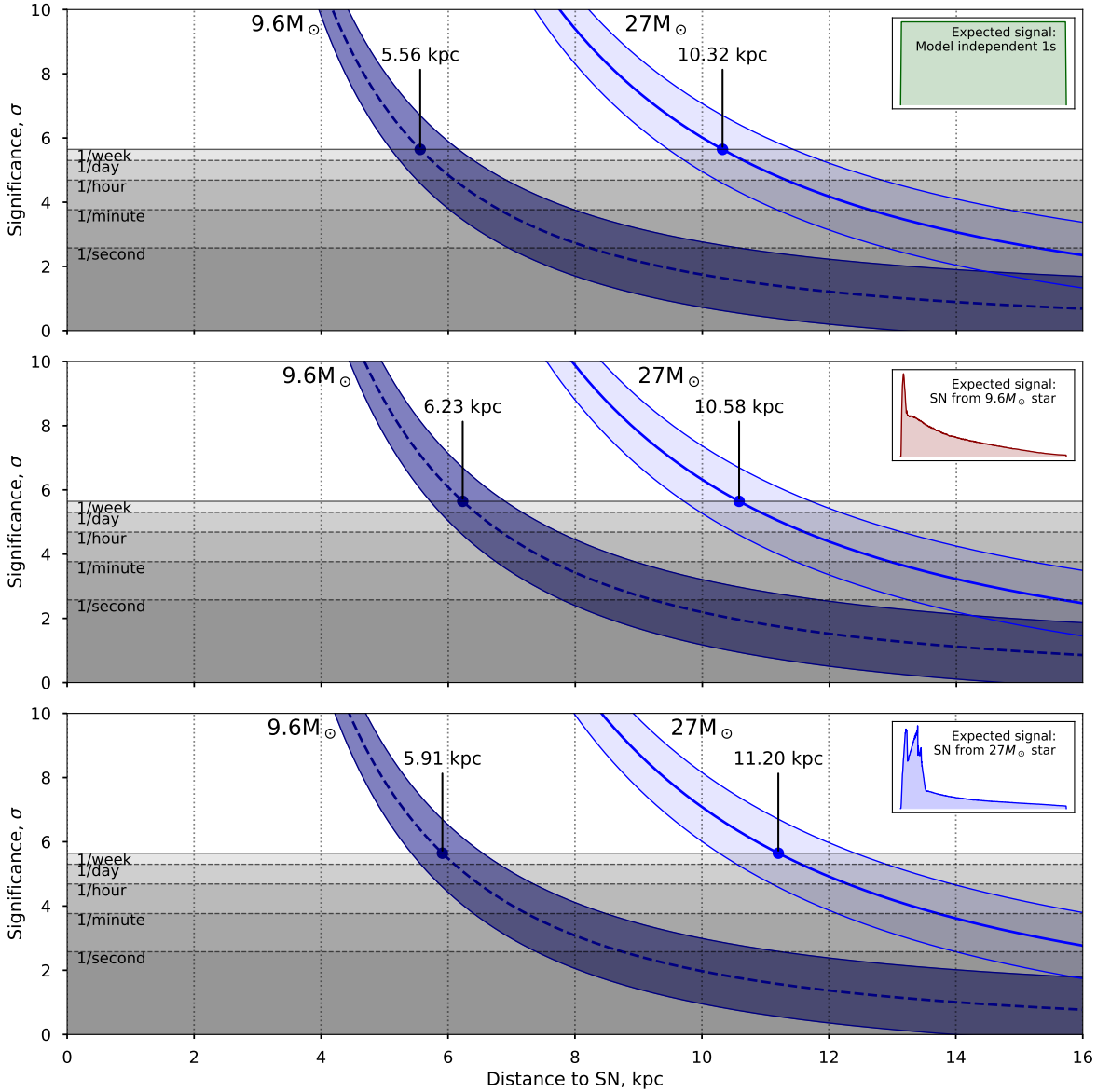

Efficiency vs. distance in NOvA detectors

Far Detector

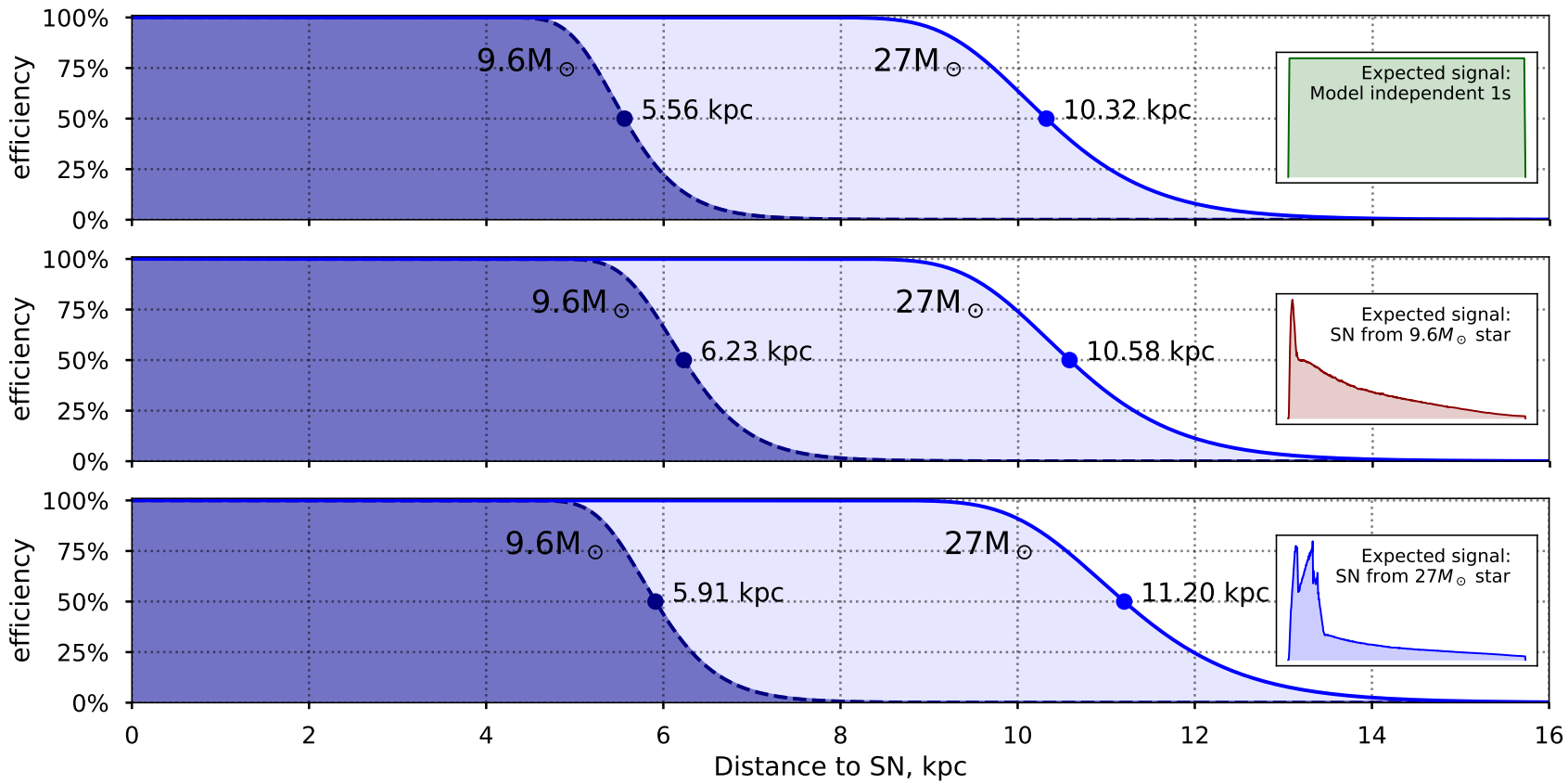

Efficiency vs. distance in NOvA detectors

Near Detector

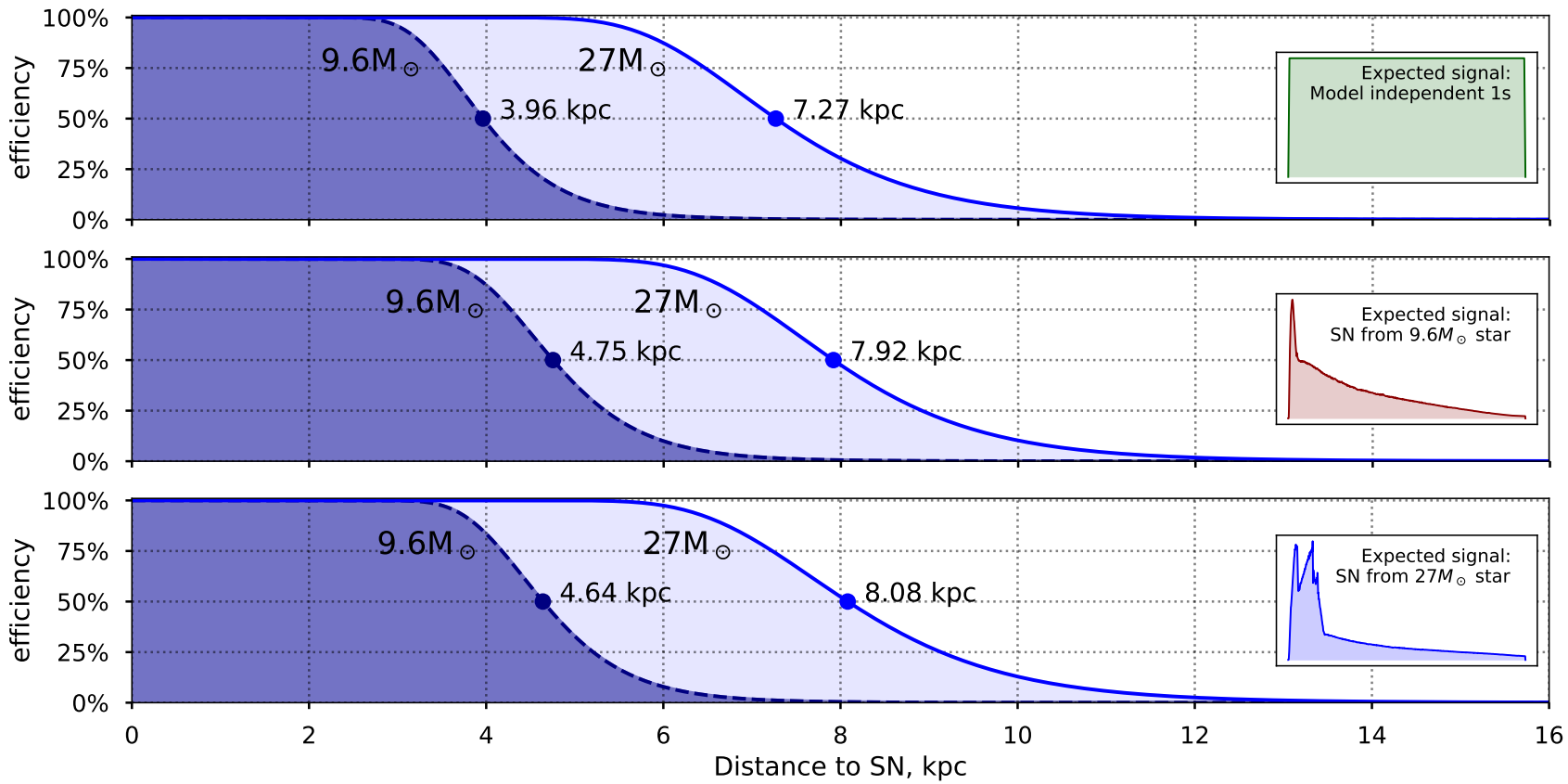

Probability to detect galactic supernova

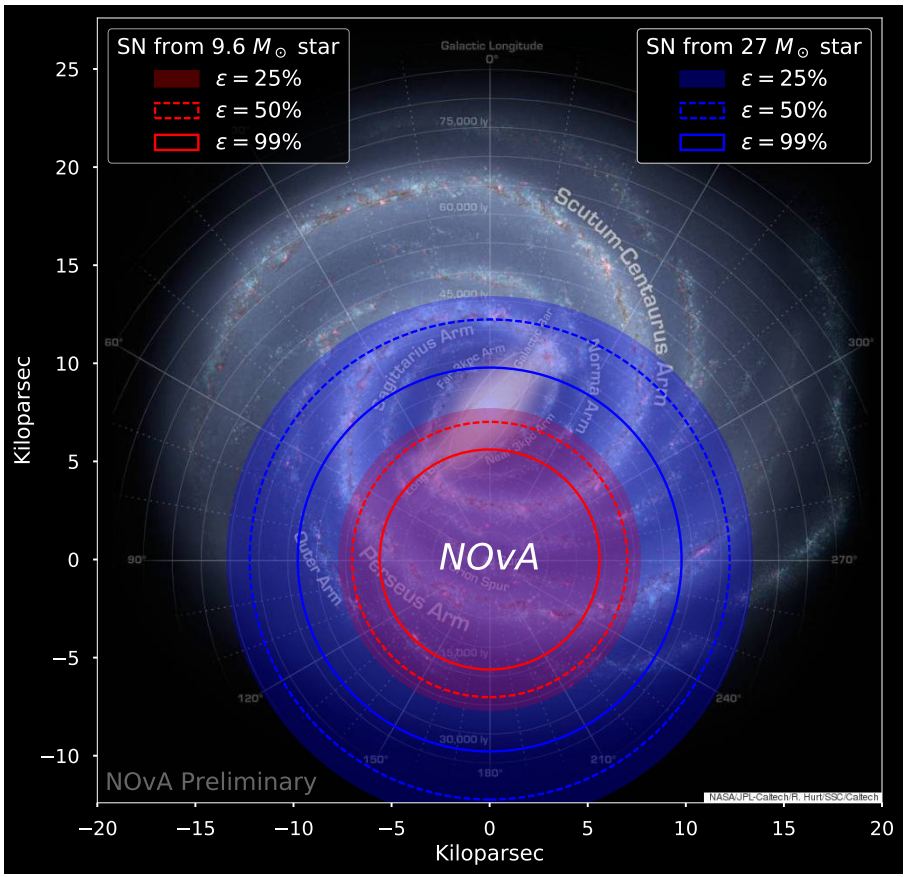

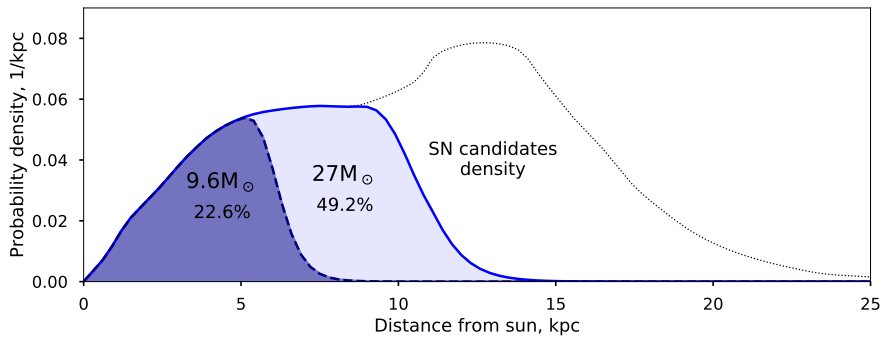

- NOvA's sensitivity covers the galactic center.
- This sensitivity is defined by Far Detector. Using Near Detector in a cross-detector trigger mode doesn't affect the sensitivity much.
- Current system configuration has a high threshold, defined by SNEWS requirements.

Alternative triggering system configuration

- Lower detection threshold $z = 5\,\sigma$
- Combine measurements of Near+Far detectors using Shape Analysis
- Take into account MSW effect on the neutrino signal
- Study the dependency of the significance on expected signal choice

Signal shapes

	Near detector	Far detector
N_{bg} /s	0.52	2483.21
N_{sg} (9.6 $\mathrm{M}_\odot$) NH	1.45	103.26
N_{sg} (9.6 $\mathrm{M}_\odot$) IH	1.81	130.34
N_{sg} (27 $\mathrm{M}_\odot$) NH	4.08	295.69
N_{sg} (27 $\mathrm{M}_\odot$) IH	3.58	260.03

Table: Background and signal event numbers for the NOvA detectors during the first second of a simulated supernova. Signal rates are based on the Garching group simulations with two progenitor masses at 10 kpc distance, for both normal (NH) and inverted (IH) neutrino mass hierarchies.

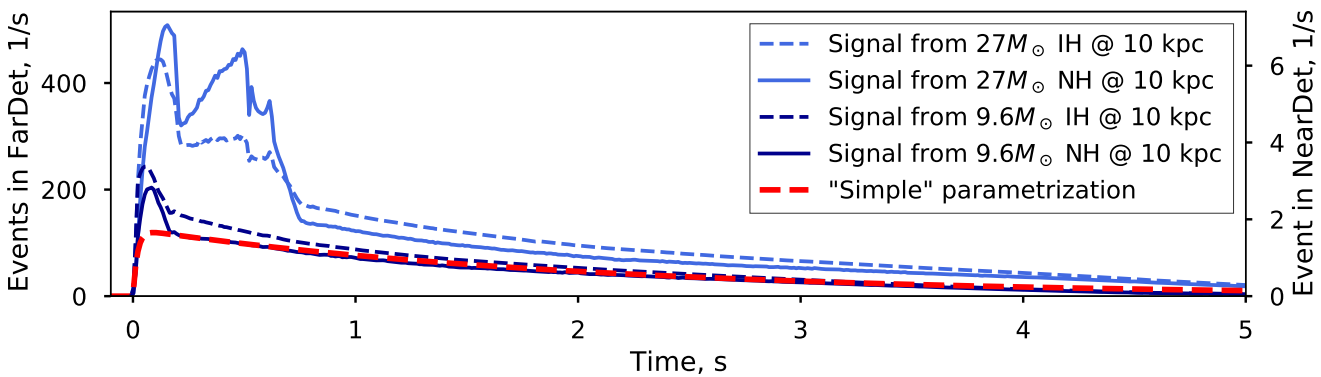

We also consider a "simple" parametrization, that roughly describes the signal tail:

$$S(t) \sim (1 - e^{-t/\tau_0}) \cdot e^{-t/\tau_1};$$

where $\tau_0 = 0.2\,\mathrm{s}$, $\tau_1 = 2\,\mathrm{s}$

Joint Near+Far sensitivity

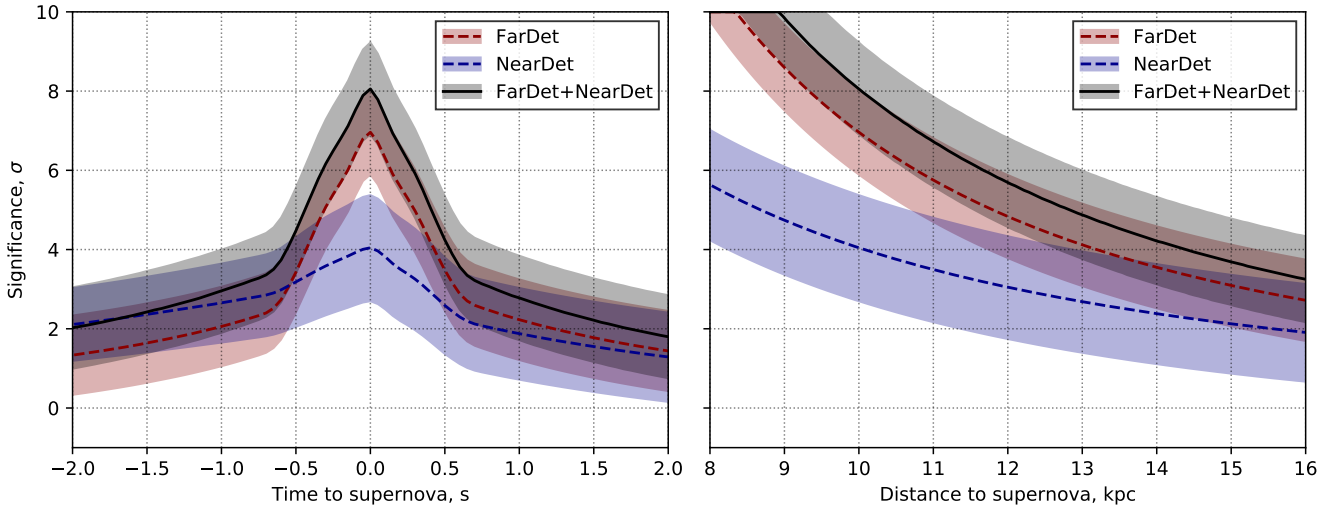

Metric	Model	Near detector CA	Near detector SA	Far detector CA	Far detector SA	Far+Near Joint SA
Distance ($\varepsilon = 50\,\%$), kpc	$27M_\odot$ IH	7.08	8.58	10.13	11.27	12.36
	$27M_\odot$ NH	7.56	8.70	10.80	11.81	12.85
	$9.6M_\odot$ IH	5.03	6.10	7.17	8.02	8.80
	$9.6M_\odot$ NH	4.50	5.47	6.38	7.18	7.89
z_{mean} at 10 kpc, σ	$27M_\odot$ IH	2.88	3.95	5.12	6.24	7.47
	$27M_\odot$ NH	2.88	4.05	5.82	6.87	8.06
	$9.6M_\odot$ IH	1.30	2.29	2.58	3.00	3.95
	$9.6M_\odot$ NH	1.30	1.92	2.04	2.30	3.20

Estimating supernova signal start time

Significance $z(t^*)$ measures goodness of fitting given data with a signal, starting at time t^*.

$$t^*_{rec} = \underset{t^*}{\operatorname{argmax}}\, z(t^*, \{t_i\})$$

is an estimator for the actual starting time for the signal.

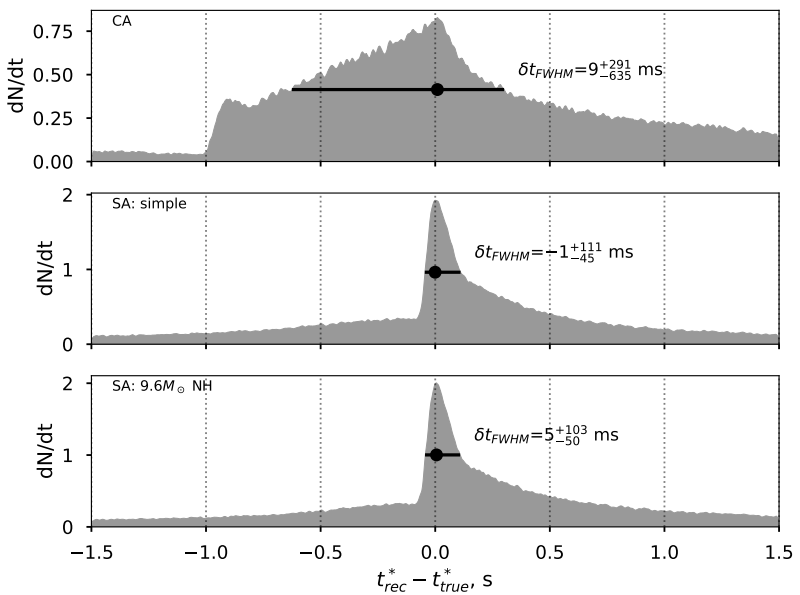

Figure: Distribution of the supernova start time estimation error $t^*_{rec} - t^*_{true}$ for the simulated samples of neutrino interactions from $9.6\,\mathrm{M}_\odot$ NH at $d = 10\,\mathrm{kpc}$ distance in the NOvA far detector.

We estimated time precision using Full Width at Half Maximum (FWHM) of the distributions for all combinations of expected and received signals.
Taking into account signal shape gives a ~ 5 times improvement in timing precision, even for a simple model.

Expected signal model dependency

		Analysis	Input model $27M_\odot$ IH	$27M_\odot$ NH	$9.6M_\odot$ IH	$9.6M_\odot$ NH
Distance ($\varepsilon = 50\,\%$), kpc	FarDet	CA	10.13	10.80	7.17	6.38
		simple	11.14	11.34	7.92	7.10
		$27M_\odot$ IH	**11.27**	11.62	7.96	7.14
		$27M_\odot$ NH	11.13	**11.81**	7.75	6.95
		$9.6M_\odot$ IH	11.19	11.38	**8.02**	7.16
		$9.6M_\odot$ NH	11.21	11.40	8.01	**7.18**
	NearDet	CA	7.08	7.56	5.03	4.50
		simple	8.56	8.62	6.10	5.49
		$27M_\odot$ IH	**8.58**	8.66	6.09	5.49
		$27M_\odot$ NH	8.50	**8.70**	6.00	5.41
		$9.6M_\odot$ IH	8.50	8.57	**6.10**	5.48
		$9.6M_\odot$ NH	8.49	8.58	6.08	**5.47**
z_{mean} at 10 kpc, σ	FarDet	CA	5.12	5.82	2.58	2.04
		simple	6.01	6.23	2.87	2.23
		$27M_\odot$ IH	**6.24**	6.64	3.04	2.41
		$27M_\odot$ NH	6.09	**6.87**	2.88	2.28
		$9.6M_\odot$ IH	6.08	6.30	**3.00**	2.33
		$9.6M_\odot$ NH	6.08	6.30	2.95	**2.30**
	NearDet	CA	2.88	2.88	1.30	1.30
		simple	3.93	3.98	2.27	1.90
		$27M_\odot$ IH	**3.95**	4.01	2.26	1.90
		$27M_\odot$ NH	3.91	**4.05**	2.24	1.88
		$9.6M_\odot$ IH	3.90	3.96	**2.29**	1.92
		$9.6M_\odot$ NH	3.90	3.96	2.29	**1.92**

Summary

- Current NOvA triggering system is sensitive to the supernova neutrino signal at up to 6.2 kpc for a star with a mass of 9.6 $M_\odot$ and up to 11.2 kpc for a star with a mass of 27 $M_\odot$.
- For the NOvA case, using the SA increases the maximum range of supernova detection by 1-1.5 kpc (for different supernova models) compared to the CA. The combined mode of near and far detectors will increase the detection range by another 1-1.5 kpc, compared to the individual detectors.
- The advantages over the standard event counting method are retained even when a simplified analytical waveform is used.
- Using SA increases precision of SN starting time by factor 5.

Results published in Acero et al. 2020 and A. Sheshukov, Vishneva, and A. Habig 2021.

Plan

Detectors

KamLAND

- 1 kt liquid scintillator
- IBD as delayed coincidence
- Applies series of cuts and likelihood-based selection Asakura et al. 2016
- Provides a pre-supernova significance every 15 minutes

Borexino

- 220 t (fiducial mass) liquid scintillator.
- IBD as delayed coincidence.
- Had DSNB search Agostini et al. 2021, can be applied to presupernova.
- Detection efficiency 85 % (neutron capture):

SK-Gd

- 50 kt water Cherenkov detector with Gadolinium.
- IBD as delayed coincidence, has a separate mode of detecting only neutron capture.
- Efficiency defined by the selection criteria Simpson et al. 2019.

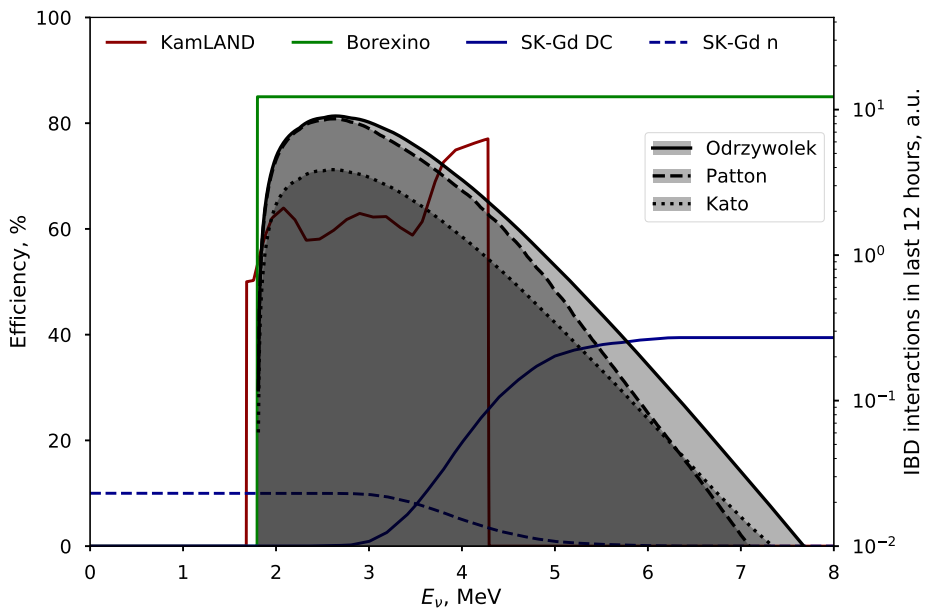

Expected signals and background

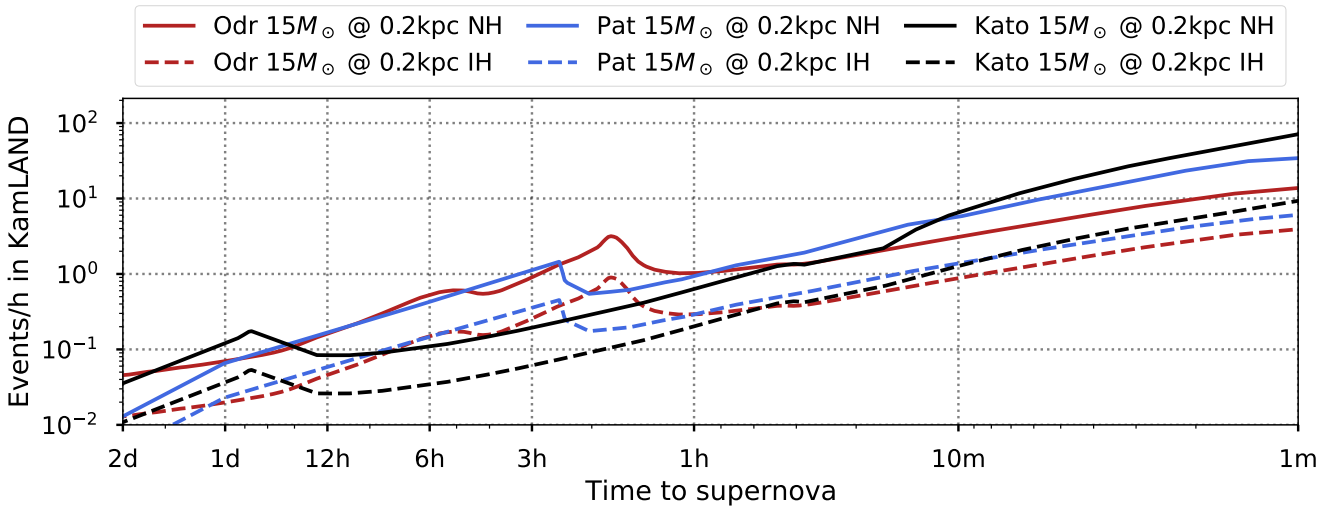

Detector	N_{sg} in the last hour before SN Kato15	Odr15	Pat15	N_{bg}/hour	Time window
Borexino	3.95 (0.705)	1.15 (0.327)	2.11 (0.5)	0.0014	48 hours
KamLAND	7.13 (1.19)	2.4 (0.681)	4.39 (1.0)	0.0029	48 hours
SK-Gd DC	86.6 (17.5)	15.7 (4.45)	29.7 (8.13)	1	12 hours
SK-Gd neutron	42.5 (7.05)	14.8 (4.21)	26.8 (6.09)	5.5	12 hours

Table: Presupernova neutrino event rates during the last hour before the supernova for the three neutrino flux models at a 200 pc distance and normal (inverted) neutrino mass hierarchy

Significance vs. time

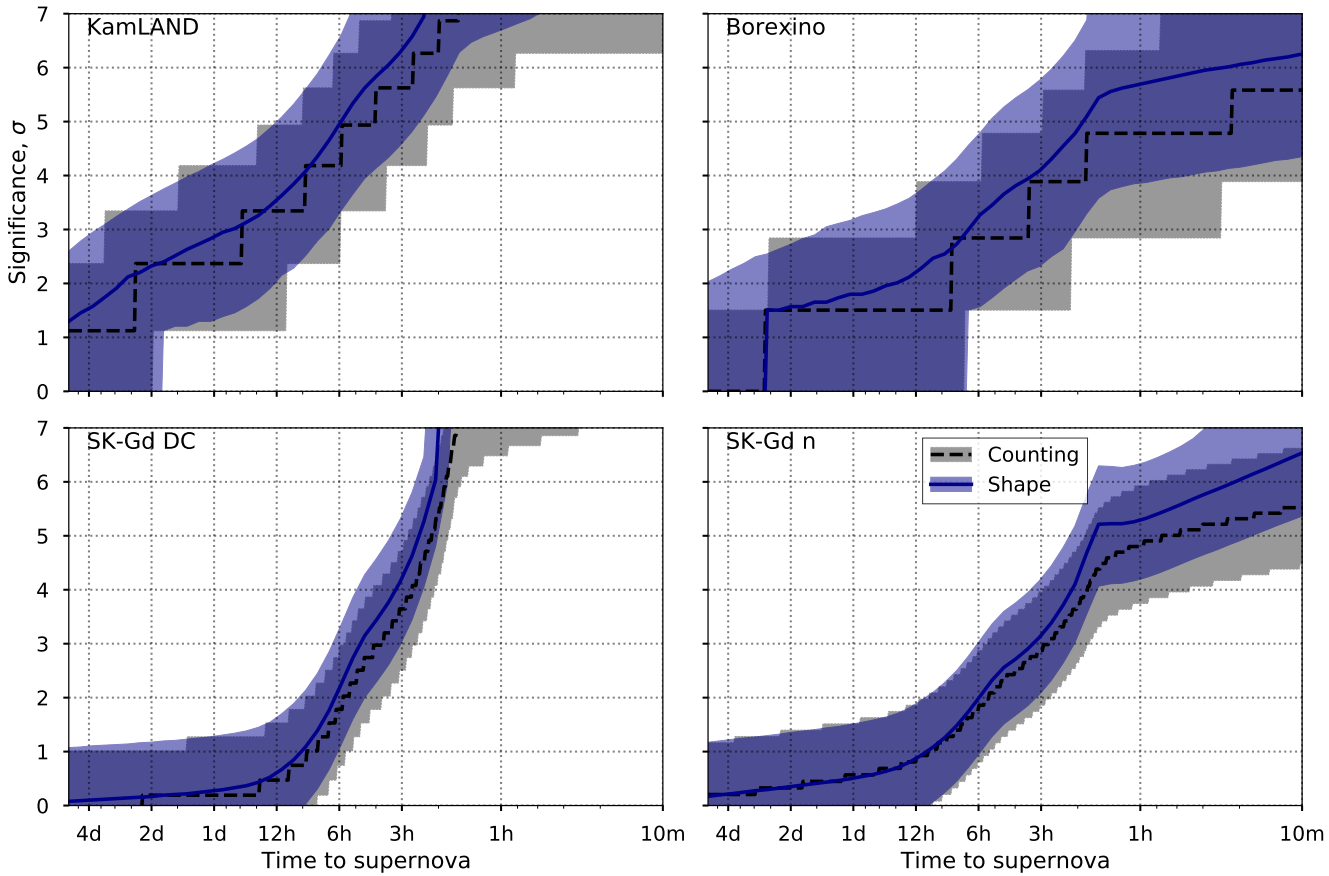

Figure: Expected significance for the various detectors using counting (dashed line) and shape (solid line) analyses for the Odrzywolek NH model at 200 pc distance vs. the time to supernova. The filled regions show the 68 % band of significance value.

Significance vs. distance

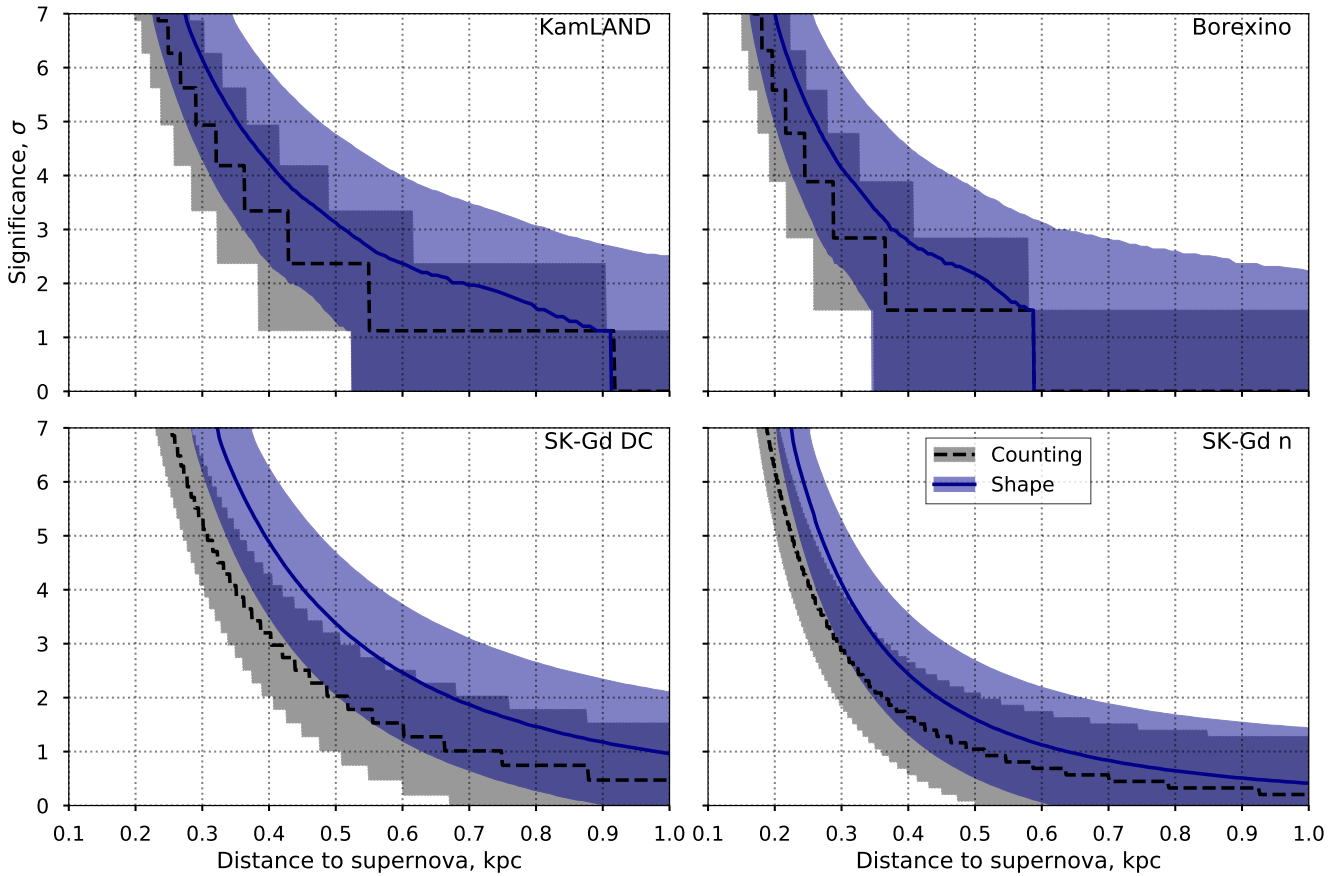

Figure: Expected significance for the various detectors using counting (dashed line) and shape (solid line) analyses for the Odrzywolek NH model 1 minute before the supernova explosion vs. the distance to supernova. The filled regions show the 68 % band of significance value.

Sensitivity regions

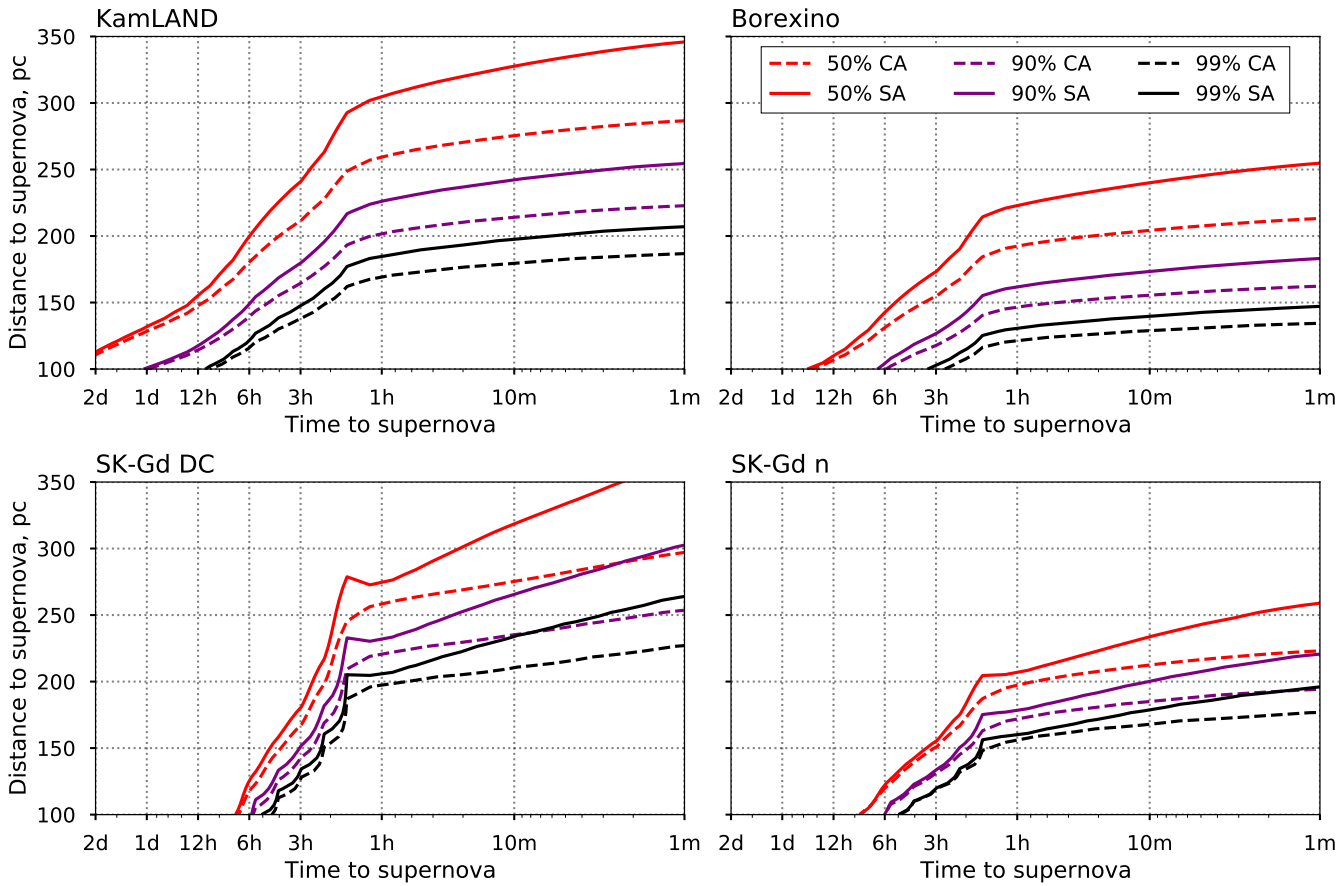

Figure: Presupernova detection reach vs. time to supernova and supernova distance with 50 %, 90 % and 99 % efficiency. The solid and dashed lines show the results of shape and counting analyses, respectively. Odrzywolek NH model is assumed for both expected and received signals.

Separate vs. joint analyses

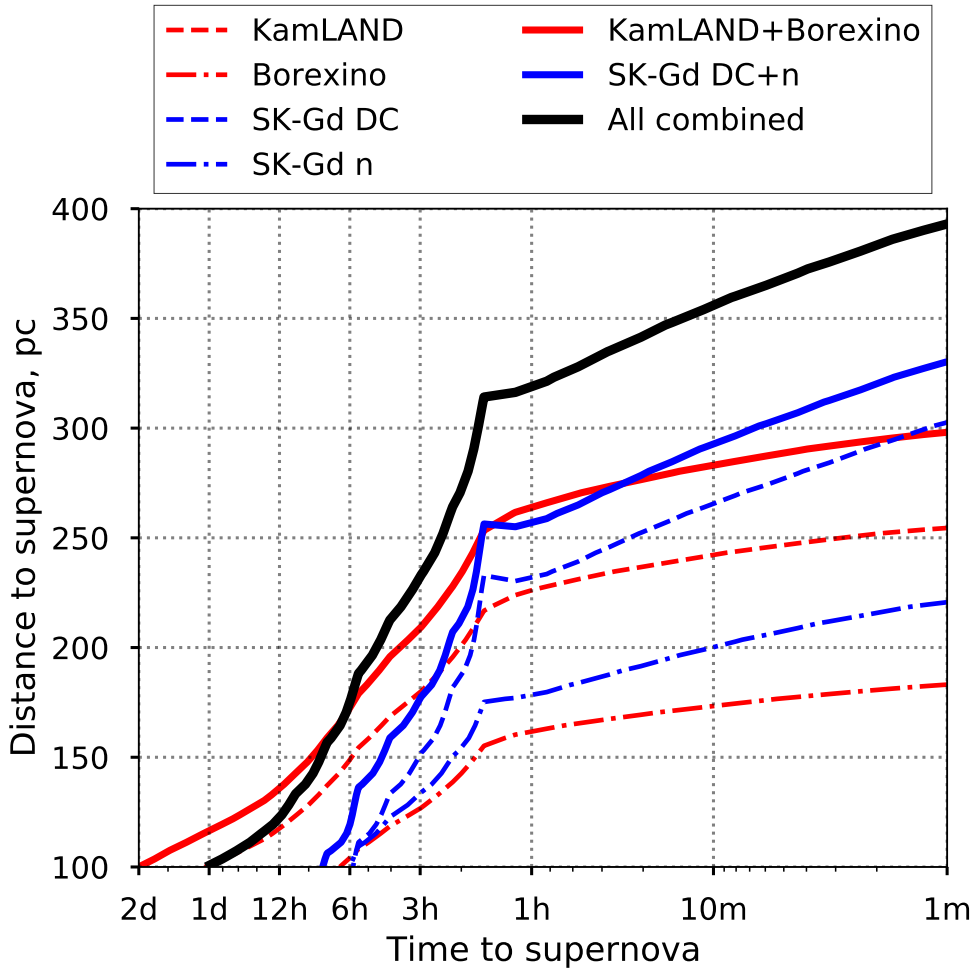

Figure: Presupernova detection reach with 90 % efficiency for the shape analyses for the individual detectors (dashed, dashdot lines) and their combinations (solid lines). Odrzywolek NH model is assumed for both expected and received signals.

Summary

- Shape analysis method is general enough to be applied for the presupernova neutrino signal.
- The sensitivity to such a signal for detectors KamLAND, Borexino and SK-Gd and their combinations is estimated.
- Shape analysis method gives advantages over the counting analysis: in the range of detection and in the time from the detection of the neutrino signal to the beginning of the collapse of the supernova core.
- For the KamLAND experiment and the significance threshold of supernova detection at 5 sigma: the maximum detection range increases by 20–60 pc and the time from detection to supernova outburst at 200 pc increases by 30–120 minutes, depending on the signal model.
- The overall sensitivity of the system increases even when adding an experiment with relatively low sensitivity. For example, for one of the considered signal models, the time from detection to supernova flare for the KamLAND+Borexino system is 500 min, significantly larger than the 239 min (KamLAND) and 21 min (Borexino) for these experiments separately.
- Obtained results don't have a strong dependency on the choice of the signal model.

Results published in A. Sheshukov, Vishneva, and A. Habig 2021

Plan

Main results of this thesis

1. A procedure for reconstruction and selection of neutrino interactions from supernovae in the Far and Near detectors of NOvA experiment has been developed. This selection procedure allowed to increase signal to background ratio by factor 35 for the Far Detector and by factor larger than 300 for the Near Detector, assuming a 9.6 $M_{\odot}$ progenitor supernova at the distance of 10 kpc.
2. A dedicated statistical Shape Analysis method was developed and applied for detecting neutrino signals from a supernova.
   The method makes is applicable both for individual detectors and for the mode of joint detection in several detectors or experiments in real time or with minimal delay.
   For the NOvA case, the method increases the maximum range of supernova detection by 1-1.5 kpc (for different supernova models) compared to the standard Counting Analysis approach. The combined mode of near and far detectors will increase the detection range by another 1-1.5 kpc, compared to the individual detectors more.
   The advantages over the standard event counting method are retained even when a simplified analytical waveform is used.
   The software package that implements the this statistical method is publicly available and can be used in other experiments.

Main results of this thesis

3. A supernova detection system based on NOvA detector data was created and launched, based on the developed reconstruction and selection procedures and statistical processing method.
   NOvA is sensitive to the neutrino signal from a supernova at up to 6.2 kpc for a star with a mass of 9.6 $M_\odot$ and up to 11.2 kpc for a star with a mass of 27 $M_\odot$.
   The system has a maximum signal detection latency of 60s.
   The system has been running on the NOvA near and far detectors since November 1, 2017. The triggering events of the system have been studied and are in line with the expected false alarm rate due to statistical background fluctuations.
4. Integration of the NOvA experiment into the global supernova search system SNEWS. The NOvA experiment is a full member of the network and is capable of sending supernova alerts to the SNEWS network. The existing infrastructure is optimized for future modifications that will be required in the development of SNEWSv2.0. The low latency of the NOvA supernova triggering system reduces the overall latency of SNEWS network for detecting the supernova signal.

Main results of this thesis

5 The developed statistical method has been applied to search for the presupernova neutrino signal. The sensitivity to such a signal for detectors KamLAND, Borexino and SK-Gd and their combinations is estimated.
Shape analysis method gives advantages over the standard method of counting events in the time window: in the range of detection and in the time from the detection of the neutrino signal to the beginning of the collapse of the supernova core.
For the KamLAND experiment and the significance threshold of supernova detection at 5 sigma: the maximum detection range increases by 20–60 pc and the time from detection to supernova outburst at 200 pc increases by 30–120 minutes, depending on the signal model.
The feasibility of using a combined analysis for several experiments is shown: the overall sensitivity of the system increases even when adding an experiment with relatively low sensitivity. For example, for one of the considered signal models, the time from detection to supernova flare for the KamLAND+Borexino system is 500 min, significantly larger than the 239 min (KamLAND) and 21 min (Borexino) for these experiments separately.

Approbation

The main results of this work were reported in the international conferences, workshops and seminars:

1. "Supernova neutrino detection in NOvA experiment" (poster), 27th International Conference on Neutrino Physics and Astrophysics (Neutrino 2016), London, Unighted Kingdom, July 2016
2. "Detection of the galactic supernova neutrino signal in NOvA experiment" (poster), 35th International Cosmic Ray Conference (ICRC 2017), Busan, South Korea, July 2017
3. "Trigger system and detection of Supernova in the NOvA experiment" (talk), 26th Symposium on Nuclear Electronics and Computing (NEC 2017), Budva, Montenegro, September 2017
4. "Detection of Galactic Supernova Neutrinos at the NOvA Experiment" (poster), 28th International Conference on Neutrino Physics and Astrophysics (Neutrino 2018), June 2018
5. "Supernova neutrino signal detection in the NOvA experiment" (talk), Workshop on Statistical Issues in Experimental Neutrino Physics (PHYSTAT-nu 2019), CERN, Switzerland, January 2019
6. "Supernova triggering and signals combination for the NOvA detectors" (talk), SNEWS 2.0 workshop: Supernova Neutrinos in the Multi-Messenger Era, Sudbury, Canada, 2019
7. "Detecting neutrinos from the next galactic supernova in the NOvA detectors" (talk), Conference on Neutrino and Nuclear Physics 2020 (CNNP2020), Cape Town, South Africa, Febaruary 2020
8. "Galactic Supernova Neutrino Detection with the NOvA Detectors" (poster), 29th International Conference on Neutrino Physics and Astrophysics (Neutrino 2020), online, June 2020
9. "NOvA in 10 minutes" (talk), Conference for young researchers in the Fermilab community (New Perspectives 2020), online, July 2020
10. "Neutrino signals of the next galactic supernova" (talk), JINR Association of Young Scientists and Specialists (Alushta 2022), Alushta, Russia, June 2022
11. "SuperNova Early Warning System v2.0" (poster), 6th International Conference on Particle Physics and Astrophysics (ICPPA 2022), November 2022

My publications

The main results of this thesis are presented in 5 publications, three of which Acero et al. 2020; Kharusi et al. 2021; A. Sheshukov, Vishneva, and A. Habig 2021 are the papers published in the journals indexed by Scopus, Web of Science, and RSCI, and two Andrey Sheshukov, Alec Habig, and NOvA collaboration 2017; SHESHUKOV 2018 are conference proceedings.

Acero, M. A. et al. (Oct. 2020). "Supernova neutrino detection in NOvA". In: *J. Cosmol. Astropart. Phys.* 2020.10, pp. 014–014. ISSN: 1475-7516. DOI: 10.1088/1475-7516/2020/10/014. eprint: 2005.07155.

Kharusi, S. Al et al. (Mar. 2021). "SNEWS 2.0: A Next-Generation SuperNova Early Warning System for Multi-messenger Astronomy". In: *New Journal of Physics* 23.3. arXiv: 2011.00035, p. 031201. ISSN: 1367-2630. DOI: 10.1088/1367-2630/abde33.

Sheshukov, A., A. Vishneva, and A. Habig (Dec. 2021). "Combined detection of supernova neutrino signals". en. In: *Journal of Cosmology and Astroparticle Physics* 2021.12. Publisher: IOP Publishing, p. 053. ISSN: 1475-7516. DOI: 10.1088/1475-7516/2021/12/053.

Sheshukov, Andrey, Alec Habig, and NOvA collaboration (Aug. 2017). "Detection of the galactic supernova neutrino signal in NOvA experiment". en. In: *Proceedings of 35th International Cosmic Ray Conference — PoS(ICRC2017)*. Bexco, Busan, Korea: Sissa Medialab, p. 958. DOI: 10.22323/1.301.0958.

SHESHUKOV, Andrey (June 2018). "Detection Of Galactic Supernova Neutrinos At The Nova Experiment". In: Publisher: Zenodo. DOI: 10.5281/ZENODO.1300755.

References I


Woosley, S. and H.-T. Janka (Dec. 2005). "The Physics of Core-Collapse Supernovae". In: *Nature Physics* 1.3, pp. 147–154. ISSN: 1745-2473, 1745-2481. DOI: 10.1038/nphys172. arXiv: astro-ph/0601261.


Janka, H.-Th et al. (Apr. 2007). "Theory of Core-Collapse Supernovae". In: *Physics Reports* 442.1, pp. 38–74. ISSN: 03701573. DOI: 10.1016/j.physrep.2007.02.002. arXiv: astro-ph/0612072.


Mirizzi, Alessandro et al. (2016). "Supernova Neutrinos: Production, Oscillations and Detection". In: *Riv. Nuovo Cim.* 39.1-2, pp. 1–112. DOI: 10.1393/ncr/i2016-10120-8. arXiv: 1508.00785 [astro-ph.HE].


Strumia, Alessandro and Francesco Vissani (2003). "Precise Quasi-elastic Neutrino/Nucleon Cross-section". In: *Physics Letters B* 564.1, pp. 42–54. ISSN: 0370-2693. DOI: https://doi.org/10.1016/S0370-2693(03)00616-6.


Marciano, William J and Zohreh Parsa (Oct. 2003). "Neutrino–electron Scattering Theory". In: *Journal of Physics G: Nuclear and Particle Physics* 29.11, pp. 2629–2645. DOI: 10.1088/0954-3899/29/11/013.


Armbruster, B et al. (1998). "Measurement of the Weak Neutral Current Excitation $^{12}C(\nu_\mu, \nu'_\mu)^{12}C^*(1^+, 1; 15.1\,MeV)$ at $E_{\nu_\mu} = 29.8\,MeV$". In: *Physics Letters B* 423.1, pp. 15–20. ISSN: 0370-2693. DOI: https://doi.org/10.1016/S0370-2693(98)00087-2.


Sheshukov, Andrey (May 2021). *Supernova statistical analysis package: sn_stat*. Version v0.3.2. DOI: 10.5281/zenodo.4782091.


Asakura, K. et al. (Feb. 2016). "KamLAND sensitivity to neutrinos from pre-supernova stars". en. In: *ApJ* 818.1. Publisher: American Astronomical Society, p. 91. ISSN: 0004-637X. DOI: 10.3847/0004-637X/818/1/91.

References II

 Agostini, M. et al. (Sept. 2021). "Search for low-energy neutrinos from astrophysical sources with Borexino". In: *Astropart. Phys.* 125, p. 102509. DOI: 10.1016/j.astropartphys.2020.102509. arXiv: 1909.02422 [hep-ex].

 Simpson, C. et al. (Nov. 2019). "Sensitivity of Super-Kamiokande with Gadolinium to Low Energy Antineutrinos from Pre-supernova Emission". en. In: *ApJ* 885.2. Publisher: American Astronomical Society, p. 133. ISSN: 0004-637X. DOI: 10.3847/1538-4357/ab4883.

Backup

Expected signal model dependency

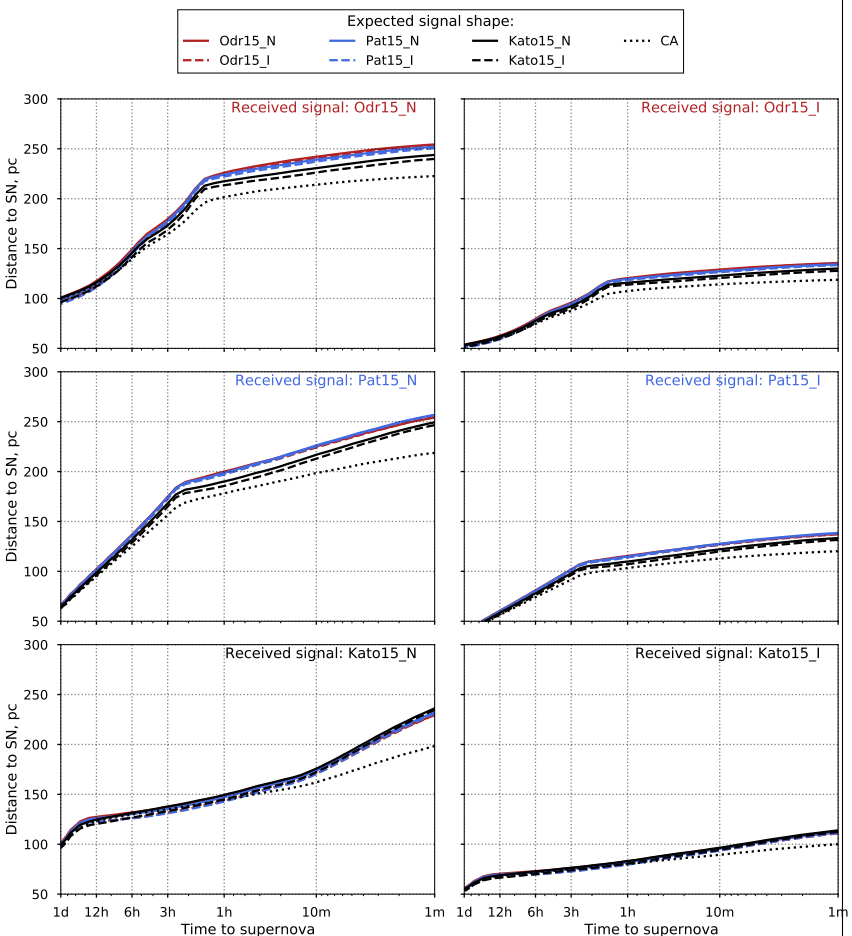

Figure: Presupernova detection reach with 90 % efficiency for the various received signals, using the shape analyses with various expected signals (solid and dashed lines) and the counting analysis (dotted lines)

Table: distance

Experiment	Analysis	Kato15		Odr15		Pat15	
		IH	NH	IH	NH	IH	NH
Borexino	CA	93.8	180.9	112.5	211.1	112.9	203.4
	SA	108.5	216.2	134.0	251.4	134.1	245.9
KamLAND	CA	125.4	242.7	151.5	284.1	152.5	274.9
	SA	146.2	293.1	182.1	341.6	183.3	336.2
SK-Gd DC	CA	122.3	236.2	155.2	291.1	150.5	272.1
	SA	170.9	345.0	188.8	354.3	180.5	336.8
SK-Gd n	CA	82.4	167.4	117.7	220.8	119.4	218.8
	SA	120.4	265.0	146.0	273.9	145.9	282.6
Borexino+KamLAND	Joint	169.9	339.9	211.0	395.9	212.0	388.9
SK-Gd DC+n	Joint	181.3	375.5	206.0	386.5	199.8	377.9
All combined	Joint	214.5	439.8	250.9	471.0	246.6	461.0

Table: Comparison of the performance of the presupernova detection for the considered detectors using the counting analysis (CA), shape analysis (SA), and for the detector combinations using the joint shape analysis (Joint). Detection threshold is $5\,\sigma$. The numbers show $d(50\,\%)$ — maximal supernova distance (in parsecs) with 50 % detection efficiency

Table: prediction time

Experiment	Analysis	Kato15		Odr15		Pat15	
		IH	NH	IH	NH	IH	NH
Borexino	CA	-	-	-	20.67	-	1.92
	SA	-	2.48	-	112.80	-	39.83
KamLAND	CA	-	16.89	-	239.25	-	183.18
	SA	-	47.75	-	355.11	-	285.07
SK-Gd DC	CA	-	3.04	-	127.69	-	51.05
	SA	-	8.57	-	149.22	-	130.97
SK-Gd n	CA	-	-	-	46.73	-	9.25
	SA	-	5.39	-	118.03	-	61.46
Borexino+KamLAND	Joint	-	280.89	12.82	500.34	7.39	408.41
SK-Gd DC+n	Joint	-	13.65	2.40	212.30	-	199.52
All combined	Joint	2.08	84.13	100.66	431.33	26.53	379.01

Table: Comparison of the performance of the presupernova detection for the considered detectors using the counting analysis (CA), shape analysis (SA), and for the detector combinations using the joint shape analysis (Joint). Detection threshold is $5\,\sigma$. The numbers $t(50\,\%)$ — amount of time to supernova (in minutes), when the presupernova signal is detected with 50 % efficiency from a 200 pc progenitor distance.

Table: significance

Experiment	Analysis	Kato15		Odr15		Pat15	
		IH	NH	IH	NH	IH	NH
Borexino	CA	1.51	4.80	1.51	5.60	1.51	5.60
	SA	2.39	6.12	2.95	6.76	3.01	6.74
KamLAND	CA	2.37	7.45	3.35	8.51	3.35	8.51
	SA	3.45	> 10	4.50	> 10	4.56	> 10
SK-Gd DC	CA	2.51	8.29	3.20	9.81	3.20	9.15
	SA	4.85	> 10	4.84	> 10	4.72	> 10
SK-Gd n	CA	0.93	4.07	1.86	6.03	1.86	6.13
	SA	2.10	> 10	2.79	9.82	2.85	> 10
Borexino+KamLAND	Joint	4.25	> 10	5.45	> 10	5.53	> 10
SK-Gd DC+n	Joint	5.21	> 10	5.57	> 10	5.50	> 10
All combined	Joint	6.65	> 10	7.68	> 10	7.67	> 10

Table: Comparison of the performance of the presupernova detection for the considered detectors using the counting analysis (CA), shape analysis (SA), and for the detector combinations using the joint shape analysis (Joint). The numbers show $z_{mean}(200\,\mathrm{pc})$ — average presupernova detection significance (in sigmas) for a 200 pc progenitor distance, 1 minute before the core collapse.